Journal of Medicinal Chemistry

Volume 49, Number 26 December 28, 2006

Perspective

Structure−Brain Exposure Relationships

Stephen A. Hitchcock* and Lewis D. Pennington

Chemistry Research & Discovery, Amgen, One Amgen Center Drive, Thousand Oaks, California 91320-1799

Received May 30, 2006

Introduction

Healthy functioning of the human brain relies on effective shielding of the sensitive neural microenvironment from potentially disruptive xenobiotic agents circulating in the periphery. The human blood−brain barrier (BBB[a]) and the blood−cerebrospinal fluid barrier (BCSFB) play essential roles in this regard (Figure 1).[1] The human BBB consists of an intricate network of capillaries estimated to be ∼600 km in length and ∼12 m^2 in surface area. These capillaries are lined with endothelial cells that are distinguished by a number of important morphological and biochemical features.[2] Notably, paracellular diffusion of molecules is highly restricted because of the lack of fenestrations and the continuous tight junctions between these cells. Active transport, both uptake and efflux, is also prevalent, as are metabolizing enzymes.[3] Energy-dependent efflux transport proteins expressed on the luminal and abluminal endothelial cell membranes recognize a wide variety of substrates and impede their access to the brain.[4] Conversely, transport proteins also ensure the uptake of essential nutrients including glucose, amino acids, vitamins, and nucleosides that otherwise would not passively diffuse into the brain. In combination, these passive diffusion, metabolic, and active transport processes present a formidable and complex biological barrier to both large- and

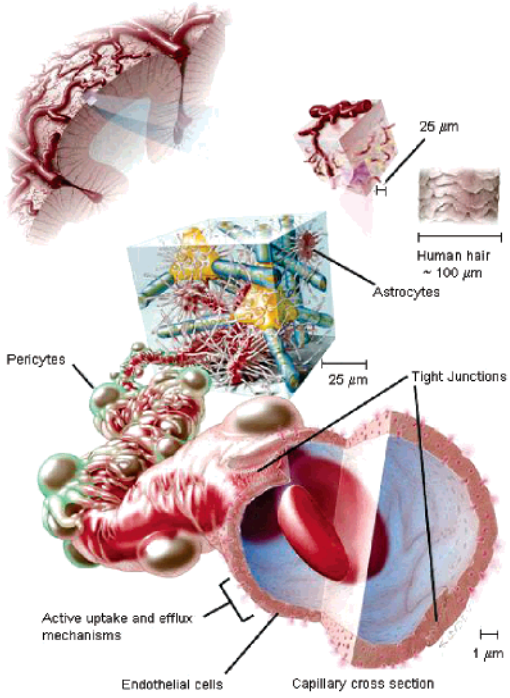

Figure 1. Blood−brain barrier. Reproduced by courtesy of and with permission from Cameron Slayden and Cosmocyte, Inc.; www.cosmocyte.com.

* To whom correspondence should be addressed. Phone: (805) 313-6041. Fax: (805) 480-3016. E-mail: stephen.hitchcock@amgen.com.

[a] Abbreviations: BBB, blood−brain barrier; BCSFB, blood−cerebrospinal fluid barrier; CSF, cerebrospinal fluid; CNS, central nervous system; CNS+/−, central nervous system penetrant/impenetrant; BBB-PAMPA, BBB parallel artificial membrane permeability assay; IAM, immobilized artificial membrane; Caco-2, human colonic carcinoma; MDCK, Madin−Darby canine kidney; BBMEC, bovine brain microvessel endothelial cells; log BB, logarithm of blood−brain partitioning; log PS, permeability-surface area coefficient; PET, positron emission tomography; SPECT, single photon emission computed tomography; HPLC, high performance liquid chromatography; AUC, area under the drug concentration−time curve; V_d, volume of distribution; $F_{u,brain}$, fraction of unbound drug in brain; log *P*, logarithm of the octanol/water partition coefficient ; clogP, calculated log *P*; log *D*, logarithm of the octanol/water distribution coefficient at a given pH ; clogD, calculated log *D*; SAR, structure−activity relationship; MW, molecular weight; HBD, hydrogen bond donors; HBA, hydrogen bond acceptors; PSA, polar surface area; B/P, brain-to-plasma ratio; Pgp, P-glycoprotein; ABC, ATP binding cassette; MRP, multidrug resistance protein; BCRP, breast cancer resistance protein; OAT, organic anion transporters; MDR, multidrug resistance gene; WT, wild-type; KO, knockout; po, per oral; sc, subcutaneous; ip, intraperitoneal; iv, intravenous; icv, intracerebroventricular.

10.1021/jm060642i CCC: $33.50
Published on Web 12/05/2006

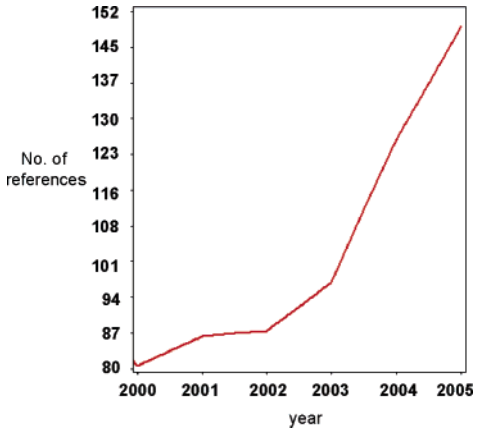

Figure 2. ACS publications from 2000−2005 that include the term "blood−brain barrier".

small-molecule entry into the brain. Since the BBB capillary network is particularly discriminating with respect to passive diffusion of molecules, it represents a major hurdle to be overcome when attempting to access targets situated within the central nervous system (CNS). For targets located in the periphery however, exclusion from the CNS may offer benefits, particularly from a side effect standpoint.

Whereas there are excellent review articles that cover many aspects of brain permeation, including the physiology of the BBB,[5] in silico methods used to predict BBB penetration,[6] and both in vitro[7] and in vivo[8] methods to estimate BBB permeability, there is a paucity of review literature dealing with aspects of BBB structure−permeability and/or structure−efflux relationships.[9] The objective of this Perspective is to review investigations reported in the past decade that illustrate the ability of medicinal chemists to use structure modification to influence BBB penetration by modulating either passive diffusion or active transport. To draw the most reliable conclusions, reports that lack in vivo data to support the effect of chemical structure on brain penetration, and provide only in vitro data or speculation, have not been included. The delivery of peptides and macromolecules across the BBB is also beyond the scope of this article, and the reader is referred to several excellent reviews of this topic.[10]

Implications of the BBB for Drug Discovery

Drugs for neurological disorders currently represent the fastest-growing segment of the pharmaceutical market, and the trend toward increasing life expectancy underscores the need to develop new drugs for age-related neurodegenerative conditions such as Alzheimer's and Parkinson's diseases. The drive to discover drugs for neurological diseases and the growing need to deliver diagnostic imaging agents and anticancer, anti-infective, and antiviral drugs to targets in the brain pose significant challenges for medicinal chemists. Although precise figures are not available, the inability of compounds to access targets located behind the BBB is a significant source of attrition in CNS drug discovery. Given the increasing economic and medical drivers for new and improved CNS and non-CNS drugs, it is not surprising that BBB permeability is attracting a heightened awareness within the pharmaceutical industry and medical fields. Within the medicinal chemistry community, the rapidly increasing importance of this topic is illustrated in Figure 2, which graphically captures the number of American Chemical Society (ACS) publications that include the term "blood−brain barrier" by publication year from 2000 to 2005.

Computational Methods for Predicting BBB Permeability

Since several excellent reviews have been published recently that describe the computational,[6] in vitro,[7] and in vivo[8] tools available for predicting, measuring, and optimizing BBB penetration, only brief mention of these techniques will be made. Roughly speaking, computational methods are divided into two types: those that classify compounds as either CNS penetrant (CNS+) or CNS impenetrant (CNS−) and those that predict the extent of BBB permeability over a continuous range of values.[11] Benefits of predictive models, including throughput and the ability to work with virtual structures, are obvious, and many promising methods have been published. The caveat associated with many computational approaches, however, is the limited amount of in vivo data that may be available to construct the models. Consequently, the pharmacological properties of marketed drugs, using disease indication and mechanism, have been used as a surrogate to imply either access to or exclusion from the CNS, an underlying assumption that may not always be correct. Extensive use of in vitro permeability data has been necessary to derive large data sets covering wider collections of compounds; however, these data are not entirely predictive of permeability in vivo.[12]

In Vitro Techniques for Predicting BBB Penetration

Though they lack the ability to reflect the influence of transport proteins, several non-cell-based, high-throughput in vitro models have been employed to estimate the potential for passive diffusion of molecules through the BBB. Among these techniques are the BBB version of the parallel artificial membrane permeability assay (BBB-PAMPA)[13] and immobilized artificial membrane (IAM) chromatography.[14] Primary cell lines such as Caco-2, Madin−Darby canine kidney (MDCK), and primary bovine brain microvessel endothelial cells (BBMEC) have become standard assays for guiding the decision-making processes in many drug discovery efforts.[7] The BBMEC model, often used with astrocyte coculture, is regarded as the most relevant of these techniques, as it more closely mimics the physiology of the BBB and is a BBB-derived cell line that provides a more realistic expression of transport proteins.[15] However, the MDR transfected MDCK cell line model has gained popularity as a system that provides a good balance between throughput, capacity, and correlation with in vivo permeability.[16] The Caco-2 cell line, typically used as a model for intestinal permeability, should be used with caution for BBB permeability prediction. Some studies[15,16] have shown that data from Caco-2 assays correlate poorly with in vivo brain transport and that the Caco-2 cell line is inferior to both MDR-MDCK and BBMEC models for in vivo predictive capability. This observation is understandable given that the BBB and the intestinal mucosa are fundamentally different biologic barriers.

In Vivo Tools for Measuring BBB Partitioning

The logarithm of blood−brain partitioning (log BB), which is simply the logarithm of the ratio of compound concentration in plasma to the concentration in the brain, is a frequently used measure of brain penetration.[2] High compound brain-to-plasma ratios (B/P), however, can often be misleading. Recent paradigm-shifting studies by Maurer,[17] Liu,[18] Summerfield,[19] and their co-workers have highlighted the importance of *free unbound* drug concentration and the pitfalls associated with simply measuring brain-to-plasma ratios of candidate molecules. Although it is well understood that albumin and α-1-acid glycoprotein are primarily responsible for plasma protein binding of

most drugs, little is known about the factors underlying brain tissue binding. Tissue binding in excess of plasma protein binding can contribute to high volume of distribution (V_d), and therefore high V_d can arguably be a harbinger of high nonspecific tissue binding. High nonspecific binding can be detrimental, as it reduces the effective drug concentration available at the pharmacological target. This aspect not only has implications for drug development but also is also particularly important in the design of radionuclide tracers (e.g., SPECT and PET),[20] for which high regional specific binding is critical for achieving high-quality images of a given target. The study by Maurer et al.,[17] using equilibrium dialysis to estimate the free fraction of 33 CNS drugs, underscored the fact that whole-brain concentration does not reflect the unbound drug concentration that is available to exert its intended pharmacological effect. These investigators suggested that the majority of the CNS drugs studied (22 of 33) freely equilibrated between blood, brain, and cerebrospinal fluid (CSF) in mice. Furthermore, in mice, unbound drug concentrations in plasma (Fu_{plasma}) approximated unbound drug concentrations in the brain (Fu_{brain}), even though the absolute brain-to-plasma ratios differed by up to 50-fold across the 22-member subset. The suggestion being that the large shifts in brain-to-plasma ratios were governed more by differences in relative nonspecific plasma and tissue binding than by BBB permeability. This point can be illustrated by comparing the data from fluoxetine with that derived from morphine. In mouse, fluoxetine has a brain-to-plasma ratio of 12 but a very low Fu_{brain} of 0.0023 and a Fu_{brain}/Fu_{plasma} of 0.074. In contrast, in mice, morphine has a lower brain-to-plasma ratio of 0.46 but has a much higher Fu_{brain} of 0.50 with Fu_{brain}/Fu_{plasma} of 1.56.

The subsequent investigation by Liu and co-workers suggested that the in situ derived permeability-surface area coefficient (log PS) and the fraction of unbound drug in brain ($F_{u,brain}$), estimated by equilibrium dialysis, can be used to model the time to reach brain equilibrium for a given compound, where rapid permeability is important.[18a] These authors argued that a permeability threshold exists for brain penetration and that optimization beyond that threshold by increasing lipophilicity may actually be detrimental, due to decreasing free unbound drug concentration. Liu and collaborators also presented the case that efforts toward optimizing brain exposure should focus on keeping intrinsic hepatic clearance low, enhancing $F_{u,brain}$ and permeability (to a threshold of ~150 nm/s in MDCK cells), as well as minimizing efflux.[18b] The recent study from Summerfield and co-workers further highlighted the role of compound free fraction and suggested that high specific binding at the pharmacological target in brain and greater free drug concentration can counterbalance poor passive diffusion and/or active efflux.[19] A potential outcome is that compounds appearing to be strong efflux substrates, or to possess modest passive diffusion in MDCK cells, can actually demonstrate meaningful brain exposure in rat. These findings illustrate the risks of relying on in vitro cell-derived efflux ratios in isolation as a selection criterion to progress compounds into in vivo studies.

With reliance on whole-brain compound concentration measurements, one additional potential pitfall should be noted: neglecting to account for the brain capillary blood volume. If residual blood is not perfused from the brain prior to homogenization and extraction of the test compound, then the amount of compound in that volume of blood must be subtracted from the total amount of compound in the brain homogenate. Since cerebral blood volume is 3−4% of the total brain homogenate, a brain-to-plasma ratio of 0.040:1 or less from non-perfused brain samples only reflects the compound concentration in cerebral blood.

The permeability surface area coefficient (log PS), typically assessed by measuring the rate of transfer of a compound from blood to brain by the short-duration in situ perfusion method, has been proposed as a more relevant indication of true permeability than a simple brain-to-plama ratio.[21] Although log PS does provide potentially valuable information on the rate of BBB permeability that may not be reflected in measured brain-to-plasma ratios, it also has the same drawback that it may also not reflect free drug concentration.

Tremendous strides have been made in recent years toward improving the sensitivity and resolution of imaging radiotracers in rodents and nonhuman primates in order to estimate both CNS penetration and biological target occupancy in the brain. The ability to nondestructively track spatial and temporal radiotracer distribution in living small animals, wherein each subject can serve as its own control, offers great advantages. However, these benefits have to be balanced against their cost, complexity, and throughput, as well as the need to work with radioisotopes. Recent published examples using HPLC coupled with triple quad mass spectrometer detection (LC/MS) to determine brain distribution of tracer compounds in rats, without resorting to radiolabeled materials, offer the promise of being able to implement a target occupancy estimation technique earlier in preclinical development.[22]

Although in vivo techniques, such as microdialysis, and in situ perfusion and tracer occupancy methods provide high-quality information, they are labor-intensive and low-throughput. Therefore, appropriate positioning of in vitro and in silico measures in the drug discovery process is usually necessary to help triage initial leads and increase the probability of success in vivo.

Physicochemical Properties that Influence BBB Permeability

The early attempts to understand the relationship between the physicochemical properties of compounds and BBB permeability focused on the role of lipophilicity. As early as 1899, Overton reported the first observations linking hydrophobic character and CNS penetration, in a study of the narcotic activity of neutral organic hypnotic agents.[23] Soloway's investigation of the influence of the addition of polar and nonpolar groups to arylboronic acids, reported in 1958, described partitioning between benzene and water as a prognosticator of a compound's BBB permeability.[24] A landmark series of studies by Hansch, starting in the late 1960s, demonstrated experimentally a parabolic relationship between log P and CNS activity in rodents and set the stage for the modern era.[25] Hansch, in attempting to quantify the role of lipophilicity, argued that CNS exclusion is favored by compounds with low log P values and, conversely, within homologous series, optimal CNS penetration occurred with compounds possessing log $P \approx 2$. An important study by Young, Mitchell, and co-workers appeared in 1988 describing a linear relationship between log BB and Δ log P, defined as log P(octanol/water) − log P(cyclohexane/water), for a series of histamine H_2 antagonists, highlighting the growing understanding of the important influence of both hydrogen-bonding capability and lipophilicity.[26]

Although lipophilicity clearly plays an important role in BBB permeability, there has perhaps been an over-reliance on optimizing this single attribute at the expense of other important considerations. For example, it is well-recognized that compound lipophilicity has a profound effect on pharmacokinetic proper-

ties.[27] High lipophilicity can contribute to excessive volumes of distribution, increased metabolic liability, and lower unbound drug concentration in the plasma and/or brain and may negatively affect pharmaceutics properties, particularly solubility. Overemphasis on lipophilicity and its effect on passive diffusion also fails to account for the influence of active transport. The importance of this process was highlighted in a recent study by Polli et al. examining the in vitro P-glycoprotein (Pgp) efflux properties of 48 marketed CNS drugs compared with 45 drugs approved for non-CNS indications.[28] By use of calcein-AM inhibition in an MDR-MDCK cell assay to determine Pgp activity, this study revealed that 72% of the combined drug sets were not substrates for Pgp. However, of the remaining 28% of drugs in the sample set that did show Pgp activity, the CNS drug set had a 7-fold lower incidence than the non-CNS drugs (using a passive permeability threshold of <150 nm/s and an efflux ratio of >2.5). In fact, only two of the CNS drugs studied had a passive permeability of <150 nm/s. Interestingly, both compounds happened to be triptan-type migraine drugs for which there is debate regarding the precise location of the target serotonin receptors and the integrity of the BBB during a migraine attack. The data from this study provide insight into perhaps what is an example of "natural selection," since many of these marketed agents were developed during an era when whole-animal pharmacology was the primary driver in early-stage drug discovery. The data from this investigation also showed that the CNS and the non-CNS drug set had comparable mean molecular weights and no difference in the number of hydrogen bond acceptors (HBA). However, the CNS drug set had fewer hydrogen bond donors (HBD), lower polar surface area (PSA), higher calculated log P (clogP) values, and fewer rotatable bonds.

Although there is still much that is not understood regarding active transport at the BBB, significant progress has been made in characterizing several transport proteins, particularly those from the ATP binding cassette (ABC) family.[29] This superfamily of transporters consists of seven subfamilies (A−G) of which three (C, B, and G) have members with known functional activity at the BBB and BCSFB. The first ABC transporter to be described, and the best characterized to date, is Pgp, which is predominantly expressed in the luminal membrane of brain capillary endothelial cells. Pgp also operates at the apical membrane of the choroid plexus, presumably to pump substances into the CSF. Multidrug resistance protein (MRP), breast cancer resistance protein (BCRP), and organic anion transporters (OATs) also have been shown recently to function at the BBB.[30] The small multidrug resistance (MDR/mdr) gene family encodes Pgp; rodents possess three gene products (mdr1a, mdr1b, and mdr2) and humans have two (MDR1 and MDR2). Only human MDR1 and rodent mdr1a/1b gene products confer drug efflux, with rodent mdr1a operating at the BBB and mdr1b in the brain parenchyma. However, it should be noted that homology between rodent and human gene products, at the amino acid level, is only ∼80%, opening the potential for compounds to behave differently across species. The development of the mdr1a/1b knockout (KO) mouse has provided a valuable tool to assess the influence of Pgp efflux in vivo and has put into context the efflux ratios measured in cell-based in vitro assays such as Caco-2 or MDR-MDCK.[31] For example, in a recent study of CNS drugs in the mdr1a/1b KO mouse, Doran and co-workers showed that of 34 drugs tested only 7 showed no evidence of efflux, as measured by brain-to-plasma AUC values, compared to wild-type (WT) mice.[32] Fourteen of the drugs showed evidence of modest efflux (1.1- to 2.6-fold AUC differences), and three, including 4-(6-fluoro-1,2-benzisoxazol-3-yl)-1-hydroxy-1-[2-(2-methyl-4-oxo-3,4,6,7,8,9-hexahydro-2*H*-pyrido[1,2-*a*]pyrimidin-3-yl)ethyl]piperidine (risperidone), showed evidence of pronounced efflux (6.6- to 17-fold AUC differences). These data support the notion that active efflux is modest or absent in most CNS drugs but also that efflux may be counterbalanced by compensating properties such as high unbound drug concentration. It cannot be understated, however, that optimizing for reduced efflux remains an important avenue for increasing the odds of generating a CNS-active compound. Because both active uptake and efflux are governed by energy-dependent transport processes that rely on small molecule−protein interactions, it is not surprising that as in drug−biological target binding, efflux recognition is sensitive to the presentation and type of functional groups on a molecule.[33] However, unlike most drug targets, efflux processes have evolved to recognize a wide variety of substrates with immense structural diversity. This promiscuous recognition of molecules presents a formidable problem for the medicinal chemist when attempting to circumvent efflux through structure modification.

Table 1. Suggested Physicochemical Property Ranges for Increasing the Potential for BBB Penetration.

property	top 25 CNS drugs mean values	suggested limits	% of top 25 CNS drugs in suggested range	preferred range	% of top 25 CNS drugs in preferred range
PSA (Å^2)	47	<90	96	<70	76
HBD	0.8	<3	100	0−1	92
cLogP	2.8	2−5	68	2−4	52
clogD (pH 7.4)	2.1	2−5	61	2−4	61
MW	293	<500	100	<450	100

From the initial findings of the role of lipophilicity on BBB permeability, several studies, most notably from the groups of Abraham,[34] Gratton,[35] and van de Waterbeemd,[36] have attempted to capture the key physicochemical properties that influence BBB permeability. The following properties have been identified as generally having a strong influence: lipophilicity, number of hydrogen bond donors (HBD), polar surface area (PSA), and molecular size and shape, with lesser contributions from hydrogen bond acceptors (HBA). Although the role of molecular shape is not well understood, cross-sectional area (A_D) has been used as a surrogate for shape, indicating that CNS+ compounds generally have A_D < 80 Å^2. The physicochemical measures are often interdependent, and it is clearly important to consider the composite of these individual characteristics rather than each one separately. In certain instances, molecular weight can operate as a crude amalgamation of these collective properties. Table 1 provides suggested physicochemical property ranges for increasing the *probability* of attaining improved BBB permeability while balancing considerations for pharmacokinetic and pharmaceutics properties. Table 1 also indicates the mean values for the physicochemical properties of the 25 top-selling CNS drugs in 2004, as well as the percentage of those drugs that fall within the suggested ranges. Although this type of rules-based approach is clearly a simplification of the complex underlying biochemical processes and physicochemical features involved in BBB permeability, it provides useful simple guidelines for the medicinal chemist concerned with designing individual compounds or libraries with improved probability of CNS penetration.

The following case studies summarize attempts by a number of laboratories to alter passive diffusion or active transport through the rational modification of chemical structure. Optimization for improved passive diffusion is covered in the first portion of the review and includes approaches mostly focused

on modulating physicochemical properties by replacing or deleting specific functional groups. For example, carboxylic acid functionality, because of its high polarity and negative charge at physiological pH, has generally been perceived to be troublesome for BBB permeability. This segment is followed by a discussion of prodrugs. Sections on approaches to exploit active uptake mechanisms and on mitigation of active efflux then conclude the article. It should become apparent that, while optimizing for BBB permeability properties, the complex challenges of maintaining potency and selectivity for the biochemical target as well as favorable pharmacokinetic properties are frequently encountered. It is hoped these examples will also illustrate the relative degree to which functional group changes influence BBB permeability within a chemical series. Calculated physicochemical values for compounds have been included in the figures to facilitate the analysis of how changes in chemical structure influence BBB permeation.[37]

Optimizing Passive Diffusion

Over the past decade, most published efforts toward optimizing the partitioning of small molecules at the BBB have focused on modulating passive diffusion. The most widely exploited avenue for altering passive diffusion has been modifying compound polarity, often using PSA and/or log *P* for predicting and rationalizing brain penetration. These measures and others are discussed in the following case studies that exemplify recent efforts to improve passive diffusion by modifying chemical structure. Unfortunately, in all but a few cases, there is no information related to the active transport properties of compounds. It is therefore often difficult to dissect out the relative contributions of passive diffusion and active transport as brain exposure varies with chemical structure.

A potent and selective antagonist of the 5-HT_6 receptor, sulfonamide **1** (SB-271046), suffers poor brain penetration that may impede its development as a possible treatment for learning and memory disorders (Figure 3).[38] Although **1** displays good oral bioavailability and activity in centrally mediated animal models of cognition, it attains poor concentrations in the brain (B/P = 0.050:1) and is a substrate for Pgp-mediated efflux. Johnson and co-workers envisaged that by simultaneously reducing the number of hydrogen bond donors and the conformational flexibility of **1**, they could produce analogues with improved BBB penetration.[38] Extensive structure−activity relationship (SAR) investigations led to the discovery of a number of compounds displaying high affinity for the human cloned 5-HT_6 receptor expressed in HeLa cells (pK_i > 8.0). Of these compounds, **2**−**4** exhibited moderate blood clearance in rat (34−44 mL min^{-1} kg^{-1}). In a steady-state CNS penetration assay in rat (infusion of 0.30 mg kg^{-1} h^{-1} for 12 h), both **2** and **4** displayed excellent brain concentrations (B/P = 3.0:1 and 2.6:1, respectively) whereas **3** displayed a somewhat diminished concentration (B/P = 0.70:1). The authors surmised this lower brain penetration results from the extra hydrogen bond donor in **3**.

Tatsumi and co-workers recently revealed studies toward developing agonists of the α7 neuronal nicotinic acetylcholine receptors (nAChR), a potential target for schizophrenia.[39] Carbamate **5** (AR-R-17779) is a subtype-selective full agonist of the α7 receptor with modest affinity (K_i = 340 nM). Compound **6** binds with high affinity (K_i = 13 nM) to this receptor (Figure 4) but displays poor oral bioavailability. In the search for compounds possessing improved potency and brain exposure relative to **5**, these investigators designed hybrid compounds, attempting to combine the favorable features of **5** and **6**. Extensive SAR studies of heteroaryl moieties eventually led to analogue **7**. This compound exhibited potent and selective partial agonist activity toward the α7 receptor (K_i = 9.0 nM), as well as good oral bioavailability. Additionally, whereas compound **5** displayed respectable brain penetration in rat (B/P = 0.76:1), that of analogue **7** was extremely high (B/P = 59:1). This shift can be rationalized in part on the basis of the absence of a HBD in **7**, resulting in a lower PSA relative to **5**, and also the overall increase in lipophilicity of **7** as judged by its calculated log *D* (clogD = 0.57; pH 7.4) compared to that of **5** (clogD = −1.5).

Because agonists of 5-HT_3 may modulate central acetylcholine release, they may be useful for the treatment of neurodegenerative and neuropsychiatric disorders.[40] Previous studies by

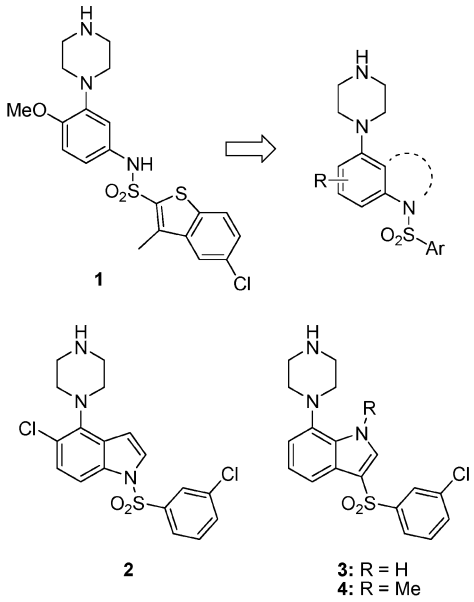

	MW	PSA (Å^2)	cLog P	cLog D	HBD	B/P
1	452	71	4.1	3.6	2	0.050
2	410	54	4.4	3.6	1	3.0
3	376	65	2.9	1.1	2	0.70
4	390	54	3.0	1.4	1	2.6

Figure 3. More conformationally rigid compounds with fewer hydrogen-bond donors, **2** and **4**, achieve higher brain-to-plasma ratios than **1** and **3**.

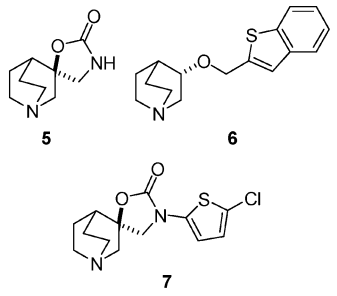

	MW	PSA (Å^2)	cLog P	cLog D	HBD	B/P
5	182	42	–0.50	–1.5	1	0.76
6	273	12	3.5	3.6	0	ND[a]
7	299	33	2.1	0.57	0	59

[a] No data.

Figure 4. The rigid and more lipophilic compound **7** is, the more brain-penetrant.

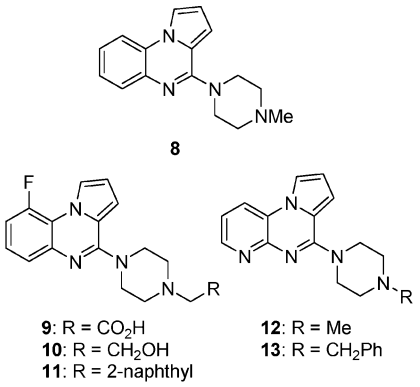

	MW	PSA (Å^2)	cLog P	cLog D	HBD	B/P
8	266	24	2.7	2.7	0	ND[a]
9	328	61	0.19	0.46	1	0.10
10	314	44	2.3	2.9	1	20
11	425	24	6.0	5.2	0	2.8
12	267	37	1.7	IC[b]	0	4.9
13	343	37	3.5	2.4	0	2.1

[a] No data. [b] Incalculable.

Figure 5. Analogue **10** may have the optimal log *P* to achieve the greatest B/P ratio.

Campiani and collaborators revealed that pyrroloquinoxalines such as **8** are high-affinity 5-HT$_3$ receptor agonists (Figure 5).[41] In order to expand the SAR and optimize binding affinity and selectivity, these workers designed and synthesized a wide variety of novel 5-HT$_3$ agonists.[40] Following affinity, selectivity, and functional efficacy assays in vitro, five compounds were selected for brain-to-plasma distribution studies. After rats were dosed with **9**−**13** (5 mg/kg iv), blood and brain samples were analyzed at 1, 2, and 3 h time points and the mean brain-to-plasma distribution ratios (AUC_t ratios) were calculated. For all of the compounds, the average brain concentrations mirrored those in plasma, suggesting that these molecules enter the brain rapidly and reach equilibrium between the brain and blood. Not surprisingly, carboxylic acid **9** displayed the highest blood and lowest brain concentrations; in fact, it was the only compound the brain concentration of which did not exceed the blood concentration (B/P = 0.10:1). Perhaps less predictably, alcohol **10** was more brain-penetrant than the more lipophilic but larger naphthane **11** (B/P = 20:1 and 2.8:1, respectively). This trend was also observed for the less lipophilic but smaller **12** compared to **13** (B/P = 4.9:1 and 2.1:1, respectively). The authors note that the plasma protein binding, which may affect the extent of brain uptake, was not evaluated.

As part of an effort to modulate the CNS permeability of the hydroxypyridinone class of iron chelators such as 3-hydroxy-1,2-dimethylpyridin-4(1*H*)-one (**14**, deferiprone), Hider and co-workers studied the effects of hydrophilic and lipophilic substituents on the core (Figure 6).[42] The extent of brain penetration of these compounds was viewed as important with regard to targeting iron overload in central versus peripheral tissues (e.g., thalassaemia). After brain perfusion for 60 s with 5.0 mM saline solutions of **14**−**22** in rats, brains were collected and the levels of the hydroxypyridinones were measured. As expected, compounds **15**−**18** and **20** penetrated the brain and there was a good correlation between BBB permeability and both log $P_{octanol}$ and log $P_{cyclohexane}$ for these simple alkyl-substituted compounds, but the *N*-hydroxyalkyl congeners **19**, **21**, and **22** did not display appreciable BBB permeability (log PS

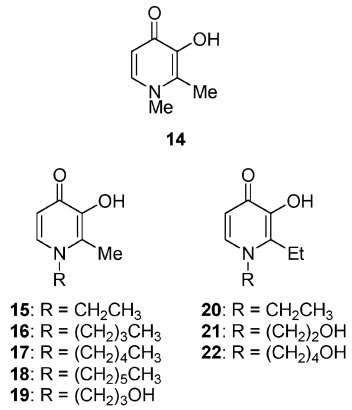

	MW	PSA (Å^2)	cLogP	cLogD	HBD	LogPS[a]
14	139	42	–0.90	–0.22	1	–1.9
15	153	42	–0.37	0.31	1	–1.5
16	181	42	0.68	1.4	1	–0.64
17	195	42	1.2	1.9	1	–0.38
18	209	42	1.7	2.4	1	–0.36
19	183	62	–1.4	–0.63	2	< –3.0
20	167	42	0.16	0.84	1	–1.0
21	183	62	–1.2	–0.32	2	< –3.0
22	211	62	–0.77	0.20	2	< –3.0

[a] Permeability–surface area coefficient.

Figure 6. Both log $P_{octanol}$ and log $P_{cyclohexane}$ are good predictors of brain permeability of simple hydroxypyridinone iron chelators **15**−**18** and **20** but not **19**, **21**, and **22**.

< −3.0). The fact that **15** and **22** have similar measured log *P* values but very different BBB permeability, suggests a significant influence of the additional HBD and the higher PSA it confers to **22**.

Smith and colleagues have sought to identify potent CNS penetrant inhibitors of serine-dependent lipase, lipoprotein-associated phospholipase A$_2$ (Lp-PLA$_2$) as potential treatments for oxidative stress arising from stroke.[43] In previous studies, they identified lipophilic 1-[(amidolinked)alkyl]pyrimidones of general structure **23** as potent inhibitors of Lp-PLA$_2$ that were poorly water-soluble (Figure 7).[44] By modification of the pyrimidone 5-substituent, they hoped to impart physicochemical properties that would improve aqueous solubility and still allow CNS penetration.[43] Following evaluation of the inhibitory activity against hLp-PLA$_2$ in rabbit and human plasma in vitro, compounds **24**−**28** were selected for BBB permeability studies. After infusion of saline solutions of **24**−**28** at a constant rate (2.0 μmol kg^{-1} h^{-1}) over 8 h to achieve steady state, analogues **25** and **27** proved to be CNS-penetrant (10% and 37%, respectively), whereas congeners **24**, **26**, and **28** were not appreciably so (≤7%). Since the compounds in this series possess high molecular weights and high PSA, it is not unexpected that **24**−**26** and **28** displayed poor or modest brain penetration. The improved CNS penetration of acid **25** and especially acid **27** is quite remarkable given that both compounds also possess high PSA and high molecular weight.

Some time ago, the Kung laboratory reported their efforts to develop novel lipophilic and neutral glucose analogues that may be useful for tumor imaging.[45] By circumventing transport via the glucose transporter and being localized by either hexokinase binding or enzyme reactions (phosphorylation), these molecules were envisioned to serve as metabolic markers of tumor cells. For this study, these workers chose to investigate the biodistributions of radiolabeled derivatives of (2*R*,3*R*,4*R*,5*S*)-2-(hy-

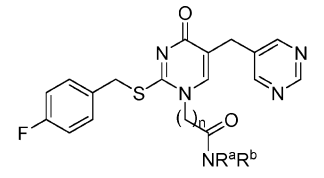

23

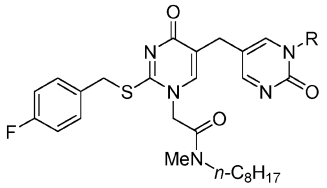

24: R = H
25: R = CH_2CO_2H
26: R = $CH_2CONHMe$

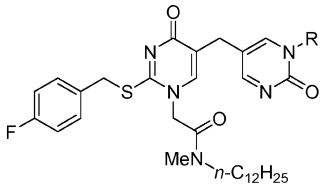

27: R = CH_2CO_2H
28: R = CH_2CO(morpholin-4-yl)

	MW	PSA (Å^2)	cLogP	cLogD	HBD	%CP[a]
24	528	101	3.1	3.6	1	7.0
25	586	127	3.7	0.99	1	10
26	599	119	3.1	3.4	1	< 7.0
27	642	127	5.8	3.1	1	37
28	711	120	5.7	6.2	0	< 7.0

[a] % CNS penetration.

Figure 7. hLp-PLA_2 inhibitors **25** and **27** are the most brain-permeable.

droxymethyl)piperidine-3,4,5-triol (**29**, 1-deoxynojirimycin) and to compare them to those of (3*R*,4*S*,5*S*,6*R*)-3-fluoro-6-(hydroxymethyl)tetrahydro-2*H*-pyran-2,4,5-triol (**30**, fluorodeoxyglucose, FDG) and its peracetylated congener **31** (AFDG) (Figure 8). Anesthetized rats were dosed with a saline solution containing 10 μCi of **30**−**35** (0.20 mL iv), sacrificed at 2, 30, 60, and 120 min time points, and then radioactivity counts of the various tissue samples were measured. As expected, the more lipophilic analogues **32** and **34** showed moderate brain uptake after 2 min (0.35 and 0.59% dose/organ, respectively), whereas their more hydrophilic counterparts **33** and **35** did not (0.030 and 0.15% dose/organ, respectively). Conversely, the hydrophilic **30** exhibited marked initial uptake (2.5% dose/organ, 2 min), whereas the more lipophilic **31** displayed only modest uptake (0.68% dose/organ, 2 min). This differential uptake was attributed to **30** being actively transported by the glucose transporter and to **31**−**35** permeating the BBB by passive diffusion. A caveat to interpreting this data is that hydrolysis of the acetylated materials in vivo may lead to an underestimation of the passive diffusion of **32** and **34** into the brain and to an overestimation of that of **31**.[45]

Kung and co-workers have also explored the development of small-molecule-based radioiodinated agents for probing in vivo the amyloid-β (Aβ) aggregates that are characteristic of Alzheimer's disease.[46] Radioiodinated styrylbenzenes **36** and **37** were based on the previously developed des-iodo congener

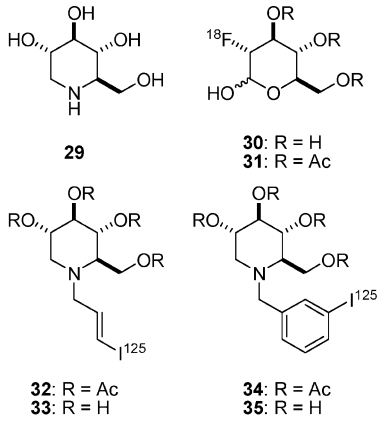

29 **30**: R = H **31**: R = Ac

32: R = Ac **33**: R = H **34**: R = Ac **35**: R = H

	MW	PSA (Å^2)	cLogP	cLogD	HBD	%BU[a]
29	163	93	–1.4	–2.8	5	ND[b]
30	181	90	–2.0	–1.3	4	2.5
31	307	108	–0.013	0.45	1	0.68
32	495	108	3.0	2.9	0	0.35
33	327	84	0.81	1.1	4	0.030
34	545	108	4.2	3.3	0	0.59
35	377	84	2.1	1.5	4	0.15

[a] % Brain uptake. [b] No data.

Figure 8. Peracetylated compounds **31**, **32**, and **34** enter the brain by passive diffusion, whereas hydrophilic congeners **33** and **35** do not appreciably cross the BBB. The sugar derivative **30** is actively transported into the CNS.

of **36** that showed excellent binding to fibrillar Aβ aggregates, whereas thioflavins **38** and **39** stemmed from a known analogue of **38** bearing methyl substituents on the nitrogen of the benzothiazole moiety as well as in place of ^{125}I (Figure 9).[46] In vitro, compounds **36**−**39** demonstrated excellent binding affinities with K_d values of 0.080, 0.13, 0.060, and 0.13 nM for aggregates of Aβ_{40} and 0.15, 0.73, 0.14, and 0.15 nM for aggregates of Aβ_{42}, respectively. Biodistribution studies in mice revealed that **38** and **39** displayed excellent brain uptake (0.67 and 1.5% dose/organ at 2 min, respectively) after iv dosing, whereas those measurements for **36** and **37** were lower (0.27 and 0.14% dose/organ at 5 min). The brain uptake values are proportional to the partition coefficient values determined experimentally for **36**−**39** ($\log P$ = 1.5, 0.041, 1.8, and 2.5, respectively). Though the higher $\log P$ value measured for phenol **36** and its higher brain penetration versus methyl ether **37** may seem surprising, it likely arises from the intramolecular hydrogen bond that can form between the phenol and the carboxylate of **36**.[46] Although, in theory, **36** possesses four potential HBD groups, two of them are likely masked through intramolecular H-bonding, which would serve to significantly lower the available PSA.

Orexins-1 and -2 (OX_1 and OX_2) are G-protein-coupled receptors (GPCRs) found in the brain that may play a physiological role in feeding and regulation of blood pressure, the neuroendocrine system, and the sleep−wake cycle.[47] To further explore the role of the OX_1 receptor, Porter and colleagues sought to identify selective OX_1 receptor antagonists.[48] By use of high-throughput functional screening of an internal library against a CHO cell line expressing the human OX_1 receptor, a 1,3-biarylurea (**40**) was identified as having good affinity (Figure 10). After several rounds of SAR studies to optimize potency and selectivity for OX_1, the 1,3-biarylureas **41**−**44** were selected to determine their ability to enter the CNS. By iv infusion of

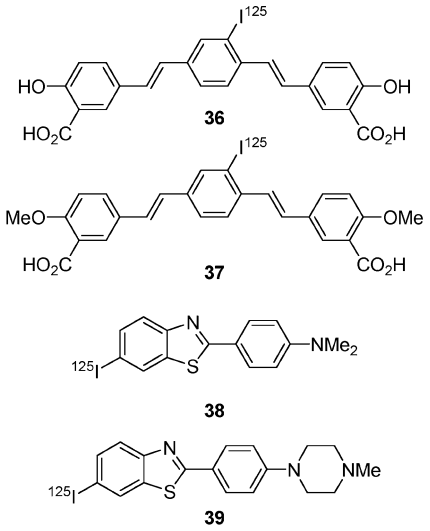

	MW	PSA (Å^2)	cLogP	cLogD	HBD	%BU[a]
36	526	115	7.9	3.6	4	0.27
37	554	93	6.8	2.1	2	0.14
38	378	16	5.6	5.7	0	0.67
39	433	19	4.8	5.0	0	1.5

[a] % Brain uptake.

Figure 9. The amyloid imaging agents **38** and **39** have greater measured log *P* values and better brain penetration than their more polar analogues **36** and **37**. Phenol **36** has greater brain uptake than methyl ether **37**.

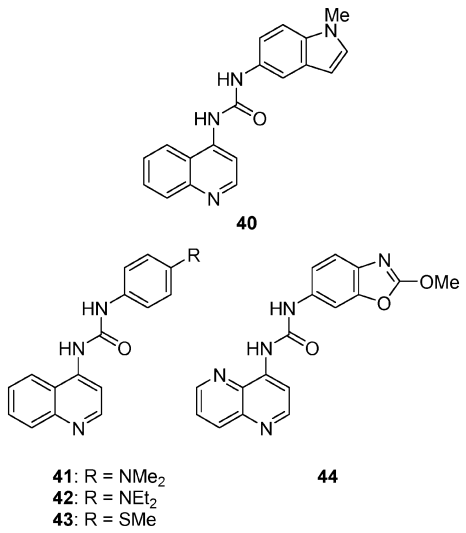

	MW	PSA (Å^2)	cLogP	cLogD	HBD	B/P
40	316	59	4.4	2.6	2	ND[a]
41	306	57	4.0	2.4	2	0.060
42	334	57	5.1	3.2	2	0.16
43	309	54	4.4	2.7	2	0.10
44	335	102	3.4	3.4	2	0.40

[a] No data.

Figure 10. The most polar compound with the potential for intramolecular hydrogen bonding, **44**, has the best brain penetration.

each drug to steady state in rat (1.8 mg kg^{-1} h^{-1} for 12 h), these workers discovered that the more lipophilic congeners **41**−**43**, having clogP values ranging from 4.0−5.1, achieved a low level of brain penetration (B/P = 0.060−0.16:1), whereas the

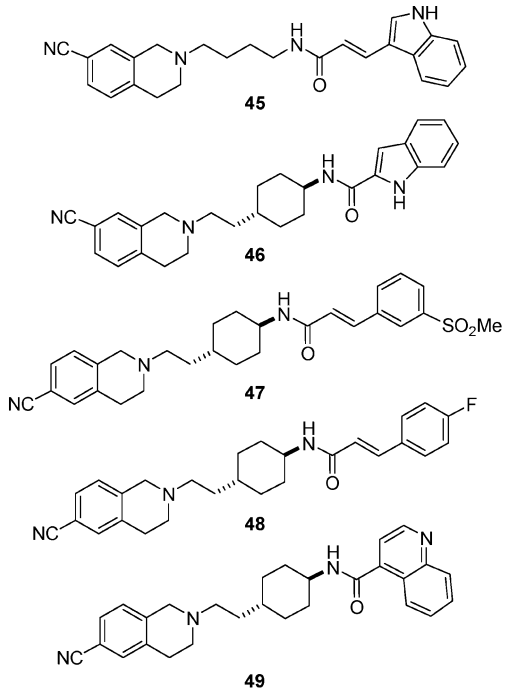

	MW	PSA (Å^2)	cLogP	cLogD	HBD	B/P
45	399	72	3.6	2.8	2	ND[a]
46	427	72	4.8	3.0	2	3.0
47	492	90	3.5	2.2	1	NG[b]
48	432	56	5.3	4.0	1	1.0
49	439	69	4.8	3.5	1	3.6

[a] No data. [b] Negligible.

Figure 11. More conformationally rigid analogues **46**, **48**, and **49** of lead molecule **45** show good brain penetration. Only the polar sulfone analogue **47** displays poor BBB permeability.

most polar analogue **44** (SB-334867, clogP = 3.4) reached a considerably higher B/P ratio (0.40:1). While these authors do not provide a rationale for this unexpected result, it is tempting to speculate that intramolecular hydrogen bonding between N5 and the proton on the proximal urea nitrogen may mask this proton donor and thereby help enhance BBB penetration.

The search for selective antagonists of the D_3-subtype of dopamine receptors D_1−D_5 has been driven by the notion that the extrapyramidal side effects of antipsychotic therapeutics operating through D_2- and D_3-subtypes arise from the D_2 activity.[49] It is therefore hypothesized that an agent selective for D_3 might maintain efficacy and possess a better side effect profile. Using brain penetration in rats as a criterion for lead optimization, Stemp and colleagues reported their efforts toward such a D_3-selective agent, leading to the discovery of cyclohexylamide **49** (SB-277011) (Figure 11).[49] From an initiative to introduce a rigidifying element in the central region of lead molecules such as **45**, early leads such as **46** emerged. Unfortunately, although **46** exhibited good affinity for D_3 and an excellent brain-to-plasma ratio in rat (B/P = 3.0:1), it also displayed inhibition of cytochrome P_{450}. Compounds in which the cyano group had been moved to C6 fared better in this regard, and compound **47** showed good bioavailability in rat. Disappointingly, **47** displayed negligible brain penetration (<2%), which may arise from the detrimental influence of the polar sulfone group which dramatically increases PSA. Further support for the problematic nature of the sulfone was provided by the good brain-to-plasma ratios exhibited by compounds that

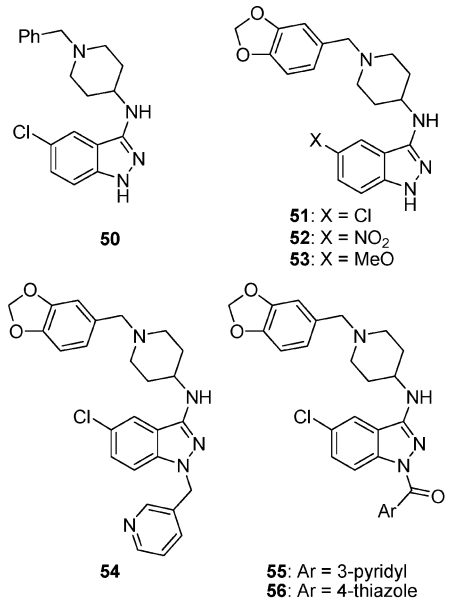

	MW	PSA (Å^2)	cLogP	cLogD	HBD	B/P
50	341	44	4.7	3.4	2	ND[a]
51	385	62	4.3	3.4	2	6.7
52	395	106	3.5	3.1	2	1.5
53	380	72	3.5	2.8	2	3.7
54	476	64	4.1	3.8	1	0.45
55	490	82	4.8	3.1	1	BQL[b]
56	496	82	4.6	3.4	1	BQL[b]

[a] No data. [b] Below the quantifiable limit.

Figure 12. Congeners **51**−**53** of lead molecule **50** exhibit good brain-to-plasma ratios. Analogues **54**−**56**, with higher molecular weights and/or greater polarity, display much poorer brain penetration.

lacked this functionality: 4-fluoro analogue **48** and quinoline **49** (B/P = 1.0:1 and 3.6:1, respectively), both of which possess significantly lower PSA and higher clogD values relative to **47**. Whether the lower brain exposure displayed by sulfone **47** is a consequence of reduced passive diffusion, efflux recognition, or some combination thereof is not clear. By microdialysis experiments in rats, **49** was later shown to block the effects of a dopamine agonist in the striatum without producing the hyperprolactinaemia often associated with D_2 activity (≥80 mg/kg po).

Melanin concentrating hormone (MCH) is an orexogenic neuropeptide that is up-regulated in fasted animals and stimulates food intake when centrally administered in mice. The MCHr1 receptor subtype in the hypothalamus has emerged as a target for treating obesity and has been the subject of extensive research in the quest for potent, selective, and brain-penetrant antagonists.[50] In this regard, Vasudevan and co-workers recently disclosed a series of MCH antagonists typified by indazole **50** (Figure 12).[50] Lead optimization of this series revealed that N-acylation and alkylation of the indazole nitrogen were well-tolerated for MCHr1 potency but had a profound effect on brain exposure and pharmacokinetic properties in diet-induced obese mice. For example, the unsubstituted indazole analogues **51**, **52**, and **53** bearing Cl, NO_2, and MeO substituents, respectively, demonstrated high exposure in both rat plasma and brain (10 mg/kg po), achieving brain-to-plasma ratios of 6.7:1, 1.5:1, and 3.7:1, respectively, based on AUC comparisons. Addition of a 3-pyridylmethyl moiety to the indazole nitrogen gave **54**, which maintained high plasma exposure but showed reduced brain

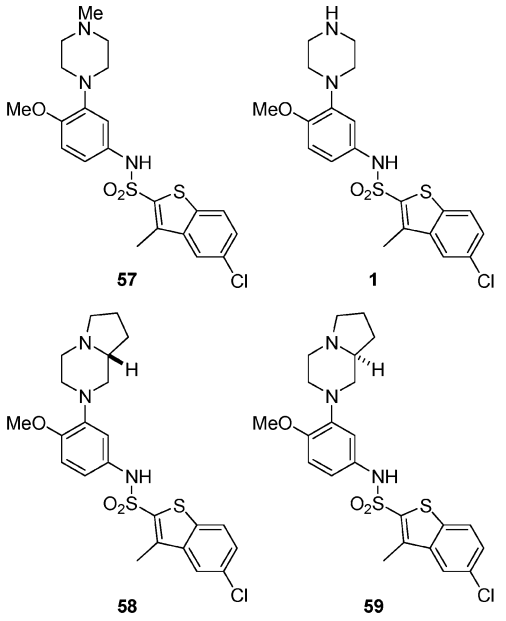

	MW	PSA (Å^2)	cLogP	cLogD	HBD	%BP[a]
57	466	62	4.4	5.4	1	18
1	452	71	4.1	3.6	2	10
58	492	62	5.8	5.0	1	ND[b]
59	492	62	5.8	5.0	1	24

[a] % Brain penetration. [b] No data.

Figure 13. Compound **59** shows improved BBB permeability versus the potentially more metabolically labile lead **57** and its N-demethylated metabolite **1**.

AUC and C_{max} compared to **51**, with a brain-to-plasma ratio of 0.45:1. In marked contrast, the N-acylated analogues **55** and **56** showed rapid clearance, gave lower plasma exposure, and most notably gave no measurable brain levels (10 mg/kg po). The greatly reduced plasma exposure of **55** and **56** (5.2- to 30-fold lower than **51**−**53**), perhaps due to the lability of the *N*-acyl groups, would be expected to consequently result in decreased brain exposure.

As we mentioned above, the 5-HT_6 receptor has been identified as a promising target for treating cognitive disorders.[38] Serafinowska and collaborators reported attempts to improve the CNS penetration of the potent and selective 5-HT_6 antagonist **57** (SB-258510), which had been shown to be efficacious in animal models of cognitive function, and its *N*-desmethyl metabolite **1** (Figure 13).[51] Following steady state infusion in rats, **57** exhibited low clearance (12.5 mL min^{-1} kg^{-1}) with modest brain penetration (18%). However, the desmethyl metabolite **1** showed equipotent affinity at the 5-HT_6 receptor but had lower brain penetration than **57**. An important point illustrated by this study is that while N-methylation of amino groups can be an effective means of reducing hydrogen bond donors and enhancing CNS penetration, N-demethylation is a facile metabolic process,[52] and the corresponding metabolites may have high exposure in the periphery relative to the CNS. Hence, efforts in this case focused on suppressing N-dealkylation. Along those lines, a number of cyclic analogues were prepared leading to enantiomeric compounds **58** and **59**, which displayed very similar 5-HT_6 affinities and selectivity profiles. Gratifyingly, in further studies **59** maintained the excellent affinity for 5-HT_6 as well as the selectivity seen with **57** but with lower potential for dealkylation. Compound **59** also

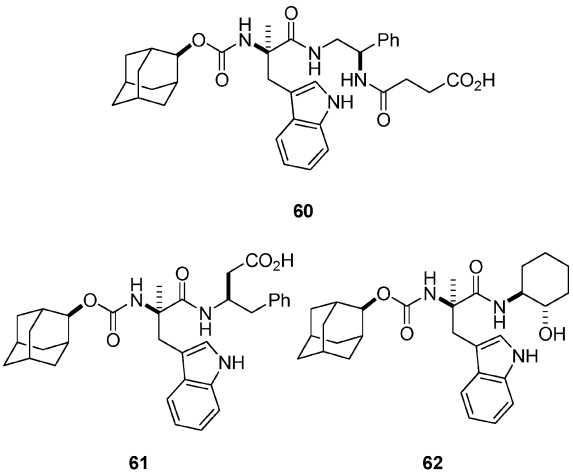

60

61 **62**

	MW	PSA (Å^2)	cLogP	cLogD	HBD	BL[a]
60	615	150	5.0	2.7	5	10
61	558	121	5.6	3.7	4	ND[b]
62	494	103	4.7	4.9	4	180

[a] Brain level (pmol/forebrain). [b] No data.

Figure 14. Possessing lower molecular weight and polarity, hydroxycyclohexylamine analogue **62** displays improved oral bioavailability and brain penetration compared to its acid congeners **60** and **61**.

provided a modest improvement in brain penetration (24%) in rat when dosed under the same conditions as **57**.

The cholecystokinin (CCK) receptor family, located both peripherally and in the CNS, has emerged as a target class for treating neuropsychiatric, anxiety, and related disorders, and a number of potent antagonists selective for the A- and B-subtypes have been discovered. However, engendering physicochemical properties in ligands for this peptide GPCR subfamily that are consistent with good brain penetration and solubility has proven to be difficult. An illustrative compound is carbamate **60** (CI-998), a CCK-B selective antagonist ($IC_{50} = 1.7$ nM) developed at Parke-Davis that was withdrawn from clinical development because of poor bioavailability, which was attributed partly to low absorption (Figure 14).[53] A second-generation effort by Trivedi and co-workers focused on reducing molecular weight and replacing the carboxylic acid group of the C-terminus fragment.[54] Extensive SAR studies revealed that although acid functionality could impart significant CCK-B potency, as evidenced by **61** ($IC_{50} = 0.15$ nM), a compromise between permeability and potency was necessary for acceptable activity in vivo. The consolidation of these properties was embodied in analogue **62** (CI-1015), a lower molecular weight compound bearing a hydroxycyclohexylamine moiety that contributed to a significantly higher log *P* while maintaining comparable potency ($IC_{50} = 3.0$ nM) versus **60** (measured log $P = 4.3$ and 2.0, respectively; although the calculated log *P* values in Figure 14 are disproportionate, the clogD values are proportionate). Compound **62** proved to be efficacious in rodent behavioral models of anxiety and a comparison of mouse forebrain levels after iv delivery (10 mg/kg) demonstrated that **62** achieved exposure levels 17- to 20-fold higher than **60** over a 5−20 min measurement period (180:10 pmol, respectively; 5 min time point). Vindicating the original hypothesis, **62** also displayed, depending on the formulation, a 2- to 5-fold increase in rat oral bioavailability.

Castro and colleagues also hypothesized that acidic functionality, in this instance a tetrazole moiety, contributed to low BBB permeability for their benzodiazepine-derived series of

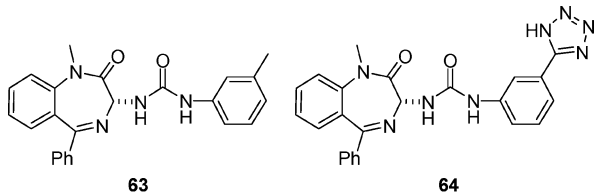

63 **64**

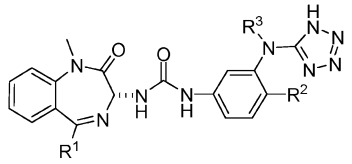

65: R^1 = Ph; R^2, R^3 = H
66: R^1 = Ph; R^2, R^3 = Me
67: R^1 = Ph; R^2, R^3 = -CH_2CH_2-
68: R^1 = CyHex; R^2 = H; R^3 = Me

	MW	PSA (Å^2)	cLogP	cLogD	HBD	ED_{50}[a]
63	398	74	3.9	4.5	2	13
64	452	128	2.3	0.97	3	ND[b]
65	467	140	1.7	0.37	4	ND[b]
66	495	132	2.6	0.67	3	ND[b]
67	494	132	2.4	0.043	3	10
68	488	132	3.0	0.012	3	1.7

[a] Ex vivo binding assay vs [^{125}I]CCK-8S. [b] No data

Figure 15. Although they have greater potency against CCK-B than lead molecule **63**, tetrazole derivatives **67** and **68**, designed for improved solubility, appear to exhibit poorer brain penetration.

CCK-B antagonists.[55] The first-generation clinical candidate, urea **63** (L-365,260), suffered from poor solubility, and subsequent efforts to incorporate solubility-enhancing groups led to tetrazole **64** (L-368,730), which had the unfortunate and unintended consequence of curtailing brain exposure (Figure 15). By installation of substituents flanking the 5-aminotetrazole group to alter bond torsion angles, derivatives such as **65**−**68** were generated wherein the tetrazole pK_a and overall log *D* at pH 7.4 were attenuated (e.g., for **65**, p$K_a = 5.1$ and log $D =$ 0.89; for **66**, p$K_a = 5.7$ and log $D = 1.6$) and further increased log *D* by switching the 6-phenyl group with a cyclohexyl moiety. However, representative compounds from this series that showed 15- to 157-fold better potency for CCK-B than did **63** failed to show substantially improved ED_{50} values in a mouse brain membrane ex vivo binding assay, leading the authors to conclude that the more potent analogues had much lower brain exposure than **63**. No mention of efflux properties was made, but it is likely that the modest attenuation of pK_a and lipophilicity was not sufficient to counterbalance the inherently high PSA values of **64**−**68** (>120 Å^2) and high hydrogen bond donor count in this series.

In the search for selective modulators of the metabatropic glutamate (mGluR) family, Pinkerton and collaborators reported the discovery of several selective allosteric modulators of the mGlu2 subtype, a potential target for CNS disorders including anxiety and schizophrenia.[56] Screening hit **69** was identified as a reasonably potent potentiator of glutamate at the mGlu2 subtype (mGlu2 $EC_{50} = 380$ nM, Figure 16). However, intracerebroventricular (icv) dosing was necessary to illicit in vivo activity, suggesting poor brain penetration of **69**. This suspicion was confirmed after ip administration of **69** in rats (B/P = 0.010:1, 20 mg/kg). Once again, attention focused on the tetrazole moiety as the culprit for poor BBB permeability. Although initial attempts to delete or replace the aryltetrazole

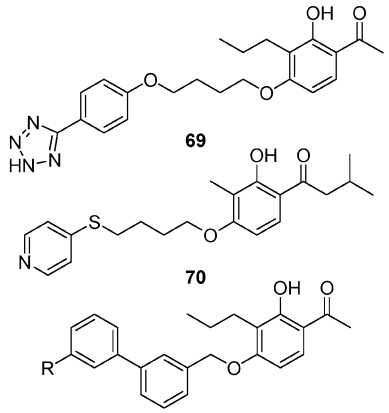

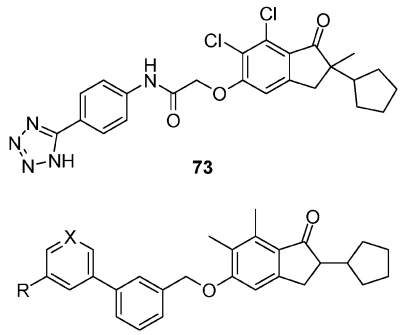

	MW	PSA (Å^2)	cLogP	cLogD	HBD	B/P
69	410	110	5.4	3.1	2	0.010
70	374	59	5.6	5.5	1	1.1
71	428	101	6.0	3.4	2	0.010
72	404	84	6.9	3.6	2	0.16
73	500	110	5.0	3.5	2	ND[a]
74	455	64	8.3	5.0	1	0.33
75	456	76	7.2	3.6	1	0.40
76	479	81	7.4	4.8	1	< 0.010
77	480	94	5.9	3.6	1	< 0.010
78	532	90	7.2	3.2	1	ND[a]

[a] No data.

Figure 16. Tetrazole compound **69** exhibits lower BBB permeability versus its thiopyridyl analogue **70**. Similarly, tetrazoles **71**, **76**, and **77** display poorer brain penetrations than their carboxylic acid congeners **72**, **74**, and **75**, respectively.

fragment with alternative five- and six-membered nitrogen heterocycles led to insufficiently active compounds, a breakthrough was realized in the form of **70**, wherein the tetrazole terminus was replaced with a 4-thiopyridyl group resulting in a 51 Å^2 drop in PSA. While exhibiting comparable potency and a modest decrease in relative potentiation compared to **69**, compound **70** gave vastly improved whole-brain levels and brain-to-plasma ratios in rat (0.40 μM and B/P = 1.1:1, respectively, at 20 mg/kg ip). In a subsequent report by Bonnefous et al., it was disclosed that further optimization of this series led to biaryl analogues **71** and **72** (EC_{50} = 73 and 400 nM, respectively).[57] Interestingly, whereas after 2 h tetrazole **71** displayed a low brain concentration (0.060 μM) and a poor

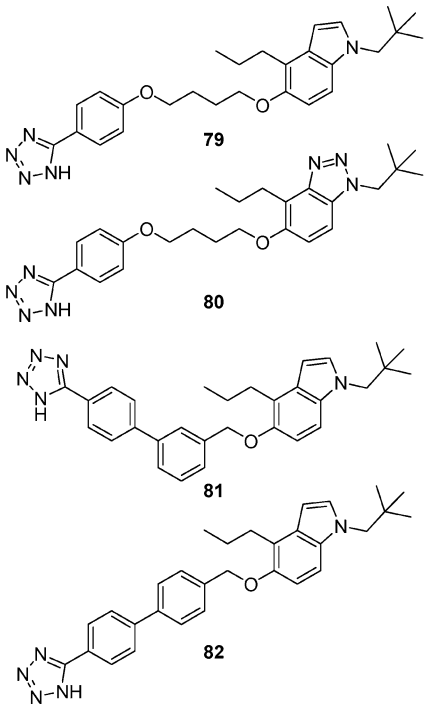

	MW	PSA (Å^2)	cLogP	cLogD	HBD	B/P
79	462	78	7.3	5.2	1	0.16
80	464	104	5.9	4.2	1	0.010
81	480	69	8.6	5.4	1	BQL[a]
82	480	69	8.6	5.4	1	BQL[a]

[a] Below the quantifiable limit.

Figure 17. *N*-Neopentylindole derivative **79** shows a better brain-to-plasma ratio than its more polar analogues keto phenol analogue **69** and benzotriazole congener **80**, as well as its higher molecular weight and more rigid biphenyl analogues **81** and **82**.

brain-to-plasma ratio in rats (B/P = 0.010:1 at 20 mg/kg ip), the carboxylic acid **72** gave remarkably improved values (0.89 μM and B/P = 0.16:1) when dosed under the same conditions. Continuation of the theme of tetrazole functionality limiting brain exposure to a greater extent than carboxylic acids is illustrated in Figure 16 with structures representing hybrids of the series derived from **71** and indanone screening hit **73**. Again, tetrazole analogues, such as **76** and **77**, gave low brain-to-plasma ratios (<0.010:1), compared to acid congeners **74** and **75** (B/P = 0.33:1 and 0.040:1, respectively). The acylsulfonamide **78** also gave poor brain levels. One would conclude from these data that replacing a carboxylic acid group with a tetrazole would be a productive means to limit CNS exposure.

In an investigation by Govek and co-workers of this class of mGlu2 potentiators, the effect of modifying the phenol functionality present in the original screening hit **69** was examined.[58] As mentioned previously, **69** displayed a poor brain-to-plasma ratio in rat (B/P < 0.010:1). In contrast, the *N*-neopentylindole derivative **79** (Figure 17) exhibited an improved brain-to-plasma ratio (B/P = 0.16:1, 2 h, 20 mg/kg ip). Interestingly, the benzotriazole congener **80**, with a PSA 28 Å^2 higher than the PSA of **79**, did not show the good CNS exposure exhibited by **79**. This observation reinforces the importance of overall molecule polarity on BBB permeability. Another informative finding was unearthed by modification of the flexible six-atom linker in this series. Though the rigidified analogues **81** and **82** maintained respectable mGlu2 potentiation (EC_{50} = 320 and 130 nM, respectively), neither displayed measurable brain levels,

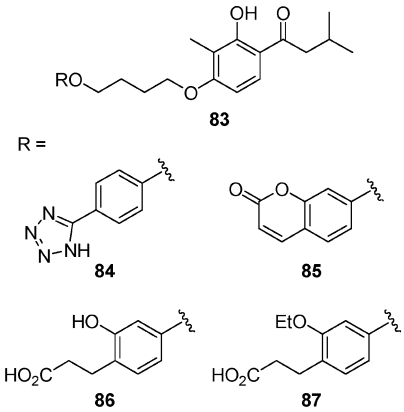

	MW	PSA (Å^2)	cLogP	cLogD	HBD	B/P
84	424	110	5.2	3.3	2	BQL[a]
85	445	113	5.5	2.9	3	ND[b]
86	473	102	6.7	3.8	2	BQL[a]
87	424	86	6.0	5.6	1	1.2

[a] Below the quantifiable limit. [b] No data.

Figure 18. Ethyl ether **87**, with lower PSA and higher clogD, is more brain-penetrant than tetrazole **84** and phenol **86**.

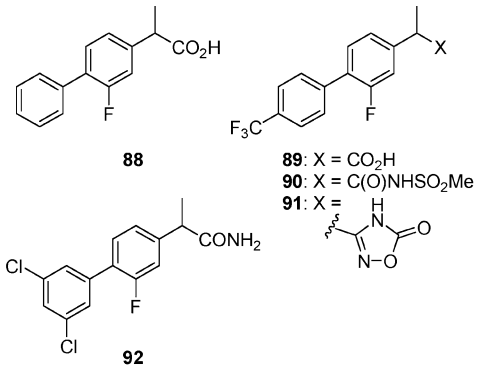

	MW	PSA (Å^2)	cLogP	cLogD	HBD	B/P
88	244	37	3.8	0.92	1	0.013
89	312	37	4.6	1.8	1	ND[a]
90	389	63	3.7	0.43	1	0.017
91	352	59	6.1	4.1	1	0.021
92	312	43	4.2	4.2	2	0.19

[a] No data.

Figure 19. Primary amide **92** shows a better B/P ratio than carboxylic acid **88**, sulfonamide **90**, and oxadiazolinone **91**, which possess lower clogD and/or higher molecular weight and polar surface area.

despite showing robust plasma exposure. While not well understood, molecule volume, shape, and flexibility are recognized as playing an important role in both intestinal and BBB permeability.[34−36] In this case, as with **69** and **7**1, it is possible that the additional phenyl group in the linker contributes negatively to passive diffusion because of a number of factors, including unfavorable shape, excessive lipophilicity, and increased protein binding.

Cube and collaborators disclosed another study in a similar series of mGluR2 potentiators typified by **83**. Replacing the aryltetrazole moiety of **84** gave a new lead compound, coumarin **85**, which subsequently led to ring-opened acid derivatives **86** and **87** (Figure 18).[59] A remarkable observation was made when comparing the rat brain exposure of these analogues. Not surprising in light of the previous data, compound **84** exhibited poor BBB permeability in rats, with no measurable brain levels after 2 h (20 mg/kg ip). Analogue **86**, which bears both phenol and acid groups, likewise exhibited undetectable brain levels, though it also displayed lower plasma exposure. Remarkably, compound **87**, wherein the phenol is capped with an ethyl group resulting in a 17 Å^2 drop in PSA, gave excellent brain levels and brain-to-plasma ratio (5.7 μM and B/P = 1.2:1). None of the compounds were Pgp substrates, indicating the brain exposure effects were a result of altered passive diffusion. Unfortunately, the brain exposure data for the comparator compound bearing the phenol but with the acid masked were not described, so it is not possible to conclude whether the poor BBB permeability of **86** is a consequence of cumulative effects of acid and phenol or whether the phenol alone would be sufficient to preclude CNS penetration. It is clear that acid functionality alone does not necessarily prohibit BBB permeability but is context-dependent. This study serves to reinforce the strong influence that hydrogen bond donors and acidic functionality can have on permeability.

The discovery that certain nonsteroidal anti-inflammatory drugs (NSAIDs) decrease the production of Aβ peptides, the amyloidogenic cleavage products of amyloid precursor protein (APP), has stimulated much interest in understanding their underlying mechanism of action.[60] It has been proposed that the Aβ-lowering effect is independent of anti-cyclooxygenase (COX) activity and acts via allosteric modulation of presenilin-1, the major component of the γ-secretase complex.[61] Accordingly, research has centered on developing improved analogues of NSAIDs by eliminating the COX activity while enhancing the inhibition of Aβ production. There has also been interest in enhancing brain permeability, in particular examining the role of the carboxyl group present in many NSAIDs. In a recent study of the influence of the acid group present in 2-(3-fluoro-4-phenyl)phenylpropanoic acid (**88**, flurbiprofen), Imbimbo and co-workers prepared a series of analogues bearing acid isosteres and measured the plasma-to-CSF ratios after a 4−7 day continuous subcutaneous infusion in rat (2−65 μg/h, Figure 19).[62] Flurbiprofen (**88**) and its closely related acid isosteres sulfonylamide **90** and oxadiazolinone **91** all exhibited very low CSF-to-plasma ratios (0.013:1, 0.017:1, and 0.021:1, respectively). However, amide analogue **92** showed a markedly improved CSF-to-plasma ratio (0.19:1), providing insight into the influence of acidic functionality and BBB permeability within this series. Interestingly, although acid isosteres **90** and **91** showed reduced inhibition of Aβ_{42} production relative to the acid **89**, amide analogue **92** appeared to have better potency against Aβ_{42} production (IC_{50} = 64 μM).

Stemming from their search for CNS-penetrant adenosine A_1 receptor antagonists, Kuroda and co-workers described another example of replacing carboxylic acid functionality to increase BBB permeability.[63] This subtype of the adenosine family of receptors is expressed at high levels in the cortex and hippocampus, and antagonists have been proposed as potential therapeutics for cognitive disorders. Fujisawa reported the discovery of the prototypical potent A_1-selective antagonists pyridazine **93** (FK838) and congener **94** (FR166124) that exert strong diuretic effects in rat but show no detectable brain exposure after oral dosing (Figure 20). In an attempt to strike a balance between increased brain permeability and metabolic stability, analogues were prepared wherein the acid was replaced with alternative, less polar functionality. Compounds were assessed for A_1 potency and selectivity, in vitro microsomal stability, and in vivo brain exposure in rat 30 min after oral delivery (10 mg/kg). The ketone **95** and tertiary alcohol **96** both

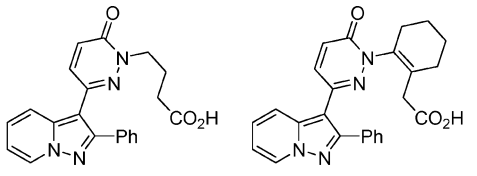

93 **94**

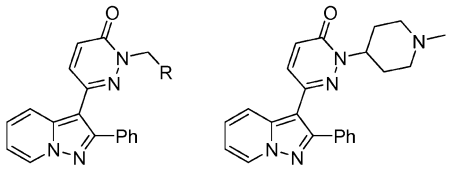

95: R = COMe
96: R = $(CH_3)_2OH$
97: R = $CONMe_2$
98: R = $CONC_5H_{10}$
99: R = $CH_2NC_5H_{10}$

100

	MW	PSA (Å^2)	cLogP	cLogD	HBD	B/P
93	374	89	1.9	IC[a]	1	BQL[b]
94	426	89	3.6	IC[a]	1	BQL[b]
95	344	69	0.87	1.4	0	0.48
96	360	72	1.7	1.7	1	0.61
97	373	73	0.28	0.84	0	0.12
98	413	73	1.1	2.3	0	BQL[b]
99	399	55	3.1	1.8	0	2.4
100	385	55	2.4	0.69	0	1.1

[a] Incalculable. [b] Below the quantifiable limit.

Figure 20. Ketone **95**, tertiary alcohol **96**, and amines **99** and **100** have improved brain penetration compared to carboxylic acids **93** and **94**, as well as tertiary amides **97** and **98**. Optimal clogP and metabolic stability seem to play a role in these differences.

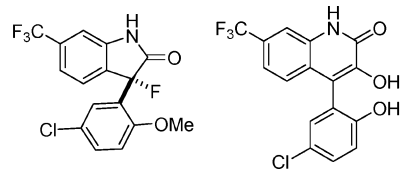

101 **102**

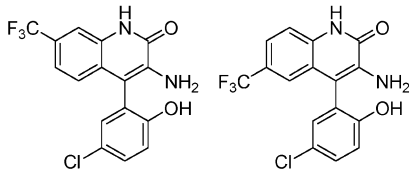

103 **104**

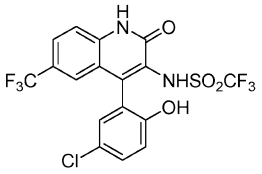

105

	MW	PSA (Å^2)	cLogP	cLogD	HBD	B/P
101	360	38	4.9	4.6	1	> 9.0
102	335	62	2.6	3.8	2	NG[a]
103	355	79	2.9	3.7	4	4.4
104	355	79	2.9	3.3	4	5.3
105	487	99	4.9	0.92	3	BQL[b]

[a] Negligible. [b] Below the quantifiable limit.

Figure 21. Amines **103** and **104** exhibit better brain penetrations than ionizable hydroxyl analogues such as **102** and sulfonamide **105**, which also have higher molecular weight and polar surface area.

delivered excellent potency for A_1 and selectivity versus A_{2A}, whereas the amides **97** and **98** and amines **99** and **100** were 1−2 orders of magnitude less potent. Interestingly, ketone **95** and teriary alcohol **96** also gave similar metabolic stabilities against rat microsomes in vitro, as well as similar plasma and brain exposures in rats after 30 min (B/P = 0.48:1 and 0.61:1, respectively). The tertiary amides **97** and **98** gave remarkably different results, with **97** displaying robust plasma exposure but a reduced brain-to-plasma ratio (B/P = 0.12:1) when compared to the ketone and tertiary alcohol analogues **95** and **96**, perhaps as a consequence of the increased polarity of the amide as gauged by its lower clogP (0.28). Amide **98** gave poor plasma exposure, perhaps as a consequence of the low metabolic stability and, most notably, gave no measurable brain level at the 30 min time point. In contrast, the more lipophilic amine analogue **99** (clogP = 3.1), which also had poor metabolic stability and low plasma exposure, did display a robust brain concentration (∼0.40 μM) and brain-to-plasma ratio (B/P = 2.4:1). Likewise, *N*-methylpiperidine analogue **100** (clogP = 2.4, 32 mg/kg) also exhibited a favorable brain-to-plasma ratio (B/P = 1.1:1), as well as a much higher overall exposure, perhaps due to its enhanced microsomal stability relative to **99**. In fact, **100** was later shown to have 60% oral bioavailability in rat. This study illustrates the subtle influence of functional group polarity effects on BBB permeability and emphasizes the need to balance the potential for decreased metabolic stability that often accompanies increased lipophilicity when optimizing for improved CNS exposure.

Activators of large conductance calcium-activated potassium (maxi-K or BKCa) channels are potential therapeutics for suppressing the neurotoxic cascade initiated by stroke, as well as for migraine treatment. Starrett, Hewawasam, and collaborators described a series of oxindole BKCa openers characterized by oxindole **101** (BMS-204352) and subsequent SAR leading to 4-aryl-3-hydroxyquinolin-2-ones such as **102** (Figure 21).[64] Unfortunately, **102** is hampered by poor brain penetration, which is postulated by the authors to be linked to the 3-hydroxyl group. To test the hypothesis that replacement of the 3-hydroxyl group would improve the BBB penetration of this series, 3-amino analogues were prepared leading to congeners **103** and **104**, both of which showed respectable activation of BKCa channels expressed in *Xenopus laevis* oocytes (160% and 190% increases in mSlo current, respectively, at 30 μM). Paradoxically, analogues **103** and **104**, although having higher PSA and an additional HBD, also displayed excellent brain exposure in rat (brain concentration of 1500 ng/mL and B/P ratio of 4.4:1 and 5.3:1, respectively, 2 h after dosing 5 mg/kg iv). It is not clear whether the absence of the 3-hydroxyl group or the presence of the 3-amino group is responsible for conferring the improved BBB exposure. Compound **101**, which possesses neither group, is reported to have excellent brain exposure in rat with a B/P ratio of >9.0:1. Further derivitization of **104** to the trifluoromethylsulfonamide **105** resulted in greatly improved channel-opening activity (340% increase in mSlo current at 30 μM). However, perhaps not surprisingly, the increased PSA and acidity resulted in **105** generating no detectable brain level when dosed under the same paradigm as **103** and **104**.

Improved CNS penetration by passive diffusion may also be achieved by using prodrugs of the active agent.[65] Because cyclooxygenase (COX-2) expression is increased in the frontal

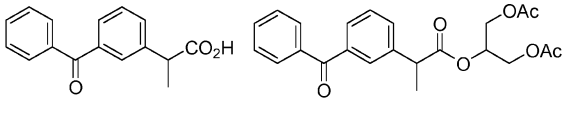

106 **107**

	MW	PSA (Å^2)	cLogP	cLogD	HBD	BUC[a]
106	254	54	2.8	–0.31	1	0.031
107	412	96	3.4	2.9	0	1.6

[a] Brain uptake clearance (mL/min/g).

Figure 22. Masking the carboxyl group of **106** to form prodrug **107** improves brain penetration.

cortex of patients suffering from Alzheimer's disease (AD), a number of researchers have investigated the hypothesis that nonsteroidal anti-inflammatory drugs (NSAIDs) might prevent neurodegeneration in AD sufferers. Deguchi and co-workers reported their efforts to enhance the brain permeability of the NSAID 2-(3-benzoylphenyl)propanoic acid (**106**, ketoprofen) by masking its carboxylic acid to give its 1,3-diacetylglyceride ester **107** (Figure 22).[66] The authors hypothesized that blocking the ionization of the carboxyl group at physiological pH and thereby increasing lipophilicity would lead to greater brain concentrations of **106**, after hydrolysis of **107** in the brain. Indeed, although **107** possesses higher PSA and molecular weight, its clogD is 2.9, compared to −0.31 for **106**.

By employing the brain metabolism index (BMI) method and the internal carotid artery infusion technique in vivo, coupled with in vitro assays, these investigators determined that **107** is rapidly hydrolyzed in both the brain capillaries and parenchymal region. Using the in situ mouse brain perfusion method, the brain uptake of **107** was measured to be 50-fold greater than **106** (1.6 vs 0.031 mL min^{-1} g^{-1}; 40 μmol kg^{-1} iv). Additionally, administration of **107** resulted in a ~3-fold increase in the area under the brain concentration−time curve of **106** compared to dosing **106** itself. Notably, the **106** produced in the CNS may be cleared by active efflux, as coadministration of probenecid, a competitive inhibitor of transport systems coupled to Na^+,K^+-ATPase, significantly increased the AUC of **106** in the brain.

The use of 9-(β-D-arabinofuranosyl)adenine (**108**, vindarabine) as a clinically efficacious antiviral and anticancer agent is constrained because of its poor aqueous solubility and facile deamination in vivo by adenosine deaminase (ADA) to its oxo metabolite **109** (Figure 23). Several years ago, Chu and co-workers endeavored to improve the pharmacokinetic properties of **108** by masking the labile amino group as an azide, giving rise to the prodrug **110**.[67] Previous studies by these investigators had revealed that azide functionality at this position in structurally similar nucleosides could serve as a metabolic precursor to an amino group by transformation via a human microsomal P_{450} NADPH-dependent system, as well as in mice.[68]

Preliminary studies in vitro, including some using murine and human liver homogenates, showed that **110** is not a substrate for ADA but is reduced gradually by the cytochrome P_{450} NADPH-dependent system to **108**.[67] Other investigations in vitro using mice liver, serum, and brain homogenates revealed that **110** had a half-life of 4.9, 3.7, and 7.3 h, respectively, in these tissues. Pharmacokinetic studies in vivo were conducted with mice. When **110** was dosed either po or iv (100 mg/kg), the half-life of **108**, produced from **110**, was found to be 7−14 times greater than for **108** administered iv. Though **108** could not be detected in the brain after its iv delivery (100 mg/kg), significant brain levels of **108** were found after **110** was administered either po or iv (0.10−0.30 μg/g from 5 to 240 min, po; from 5 to 120 min, iv). Although not studied in detail, other experiments suggested that **110** may be actively transported into the brain, as one would not anticipate such a polar compound to possess good passive diffusion characteristics.

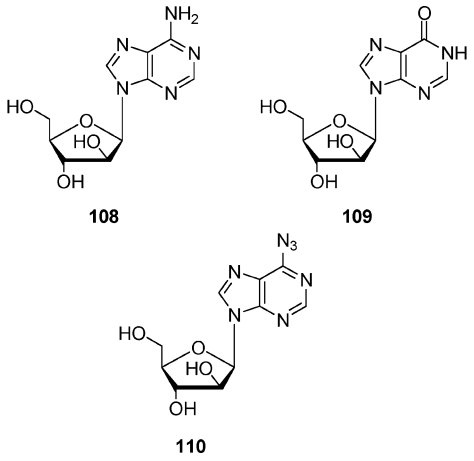

108 **109** **110**

	MW	PSA (Å^2)	cLogP	cLogD	HBD	BL[a]
108	267	140	–2.2	–1.5	5	BQL[b]
109	268	133	–3.1	–2.3	4	ND[c]
110	293	162	–0.7	–1.4	3	0.30

[a] Brain level (μg/g). [b] Below the quantifiable limit. [c] No data.

Figure 23. The azide **110** serves as a prodrug of **108** and can cross the BBB.

In contrast to the simpler prodrug approaches described above, Bodor and co-workers have developed a more complex prodrug strategy they have termed a chemical delivery system (CDS).[69] One such chemical delivery system, redox chemical delivery using dihydropyridine moieties, operates by sequential passive diffusion of the prodrug into the brain, enzymatic oxidation to form a pyridinium species, and hydrolysis to liberate the active compound. This process seeks to exploit the differential fate of the oxidized species in the central and peripheral tissues; the intermediate pyridinium compounds cannot cross the BBB and are trapped in the brain but are readily excreted by the kidney and bile, which minimizes peripheral exposure. Hydrolysis of the pyridinium compound in the brain may allow for sustained release of the active species in this tissue. One drawback of this stratagem is that the dihydropyridine prodrugs are often unstable and require parenteral delivery.

Knaus and co-workers reported an application of this approach as part of their effort to develop calcium channel antagonists (CCAs) that may be useful for controlling epileptic seizures.[70] 3-Ethyl-5-methyl-4-(2,3-dichlorophenyl)-2,6-dimethyl-1,4-dihydropyridine 3,5-dicarboxylate (**111**, felodipine) is a potent CCA and is used as a vasodilator to treat hypertension (Figure 24). These investigators envisioned that a felodipine-type CDS prodrug **112** might increase brain penetration and minimize peripheral tissue exposure of metabolite **114**, thereby increasing its anticonvulsant effects while reducing its hypertension-lowering ability. Initial experiments in vitro showed that compounds **112** and **114** displayed respectable, albeit lower, potency as calcium channel antagonists versus **111** (IC_{50} = 31, 30, and 1.5 nM, respectively).

The in vivo biodistributions of **111**, **112**, and their metabolites were measured after tail vein injection of Sprague-Dawley rats. Felodipine (**111**) achieved a maximum concentration in the brain at 5 min (5.0 μg/g, 2.5 mg/kg iv) and was undetectable after 60 min; no metabolites of **111** were detected by HPLC analysis.

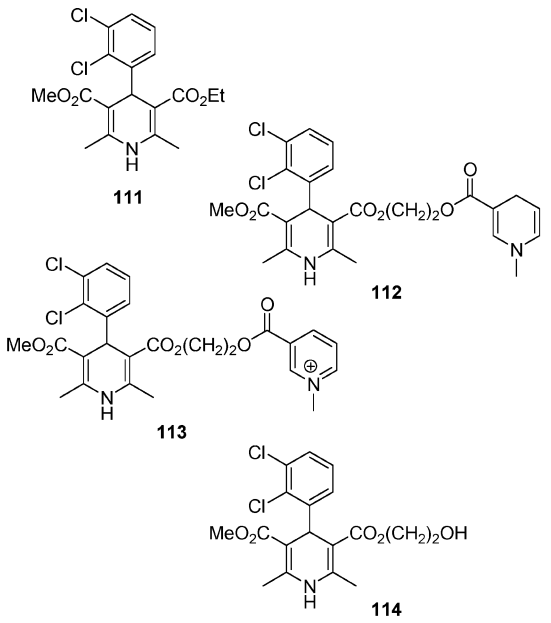

	MW	PSA (Å^2)	cLogP	cLogD	HBD	BL[a]
111	384	65	5.6	4.9	1	5.0
112	521	94	5.6	4.0	1	4.2
113	520	97	IC[b]	0.78	1	>4.0
114	400	85	4.2	3.8	2	NG[c]

[a] Brain level (μg/g). [b] Incalculable. [c] Negligible.

Figure 24. Dihydropyridine prodrug **112** readily crosses the BBB and is metabolized to pyridinium species **113**, which has a long half-life in the brain.

Though the maximum brain concentration of **112** was similar after 5 min (4.2 μg/g, 15 mg/kg iv), it had a negligible concentration after only 15 min. Interestingly, brain concentrations of its metabolite **113** remained high (>4.0 μg/g, ≥36 h) with detectable levels up to 4 days, whereas metabolite **114** remained at very low concentrations throughout the study. These investigations suggested that prodrug **112** readily enters the brain and is rapidly oxidized to pyridinium species **113**, which is then slowly hydrolyzed to **114**.

A large number of laboratories have endeavored to inhibit the aspartyl protease γ-secretase in vivo, aiming to decrease production of the pathogenic Aβ peptides that are believed to underlie Alzheimer's disease. One potential downside of inhibiting the γ-secretase that cleaves amyloid precursor protein (APP) is that it may cause undesired interference with cleavage of Notch, giving rise to toxic side effects.[71] As a possible means to circumvent this difficulty, Kraus and collaborators sought to develop prodrugs of pseudopeptide thiazolamide derivative **115** that might be more effectively delivered to the CNS and reduce the concentration of the compound in the peripheral tissues (Figure 25).[72]

Compounds **115**−**117** all show modest inhibitory activity in vitro against γ-secretase in both enzyme and cell assays (EC_{50} = 0.10−1.0 and 0.20−5.0 μM, respectively). For in vivo studies, freshly prepared samples of **115**−**117** were injected into anesthetized Sprague-Dawley rats through the jugular vein (20 mg/kg), and at various time intervals blood samples were withdrawn from the eyeballs and the brains were collected. Though all three compounds possess similar concentration and half-life profiles in blood, their rate of uptake, maximum concentration in the brain, and B/P ratios over time were markedly different. Whereas an optimal concentration of **115** in the brain was reached within 2 h (240 ng/g), this concentration was achieved by **116** (including its metabolites **115** and **117**) within only 30 min. Notably, compound **117** does not penetrate the brain but its hydrolysis product **115** was found at low concentration after 1 h (80 ng/g). After 2 h, compound **116** reached a maximum concentration in the brain (350 ng/g) and had a minimal concentration in blood (B/P > 30).

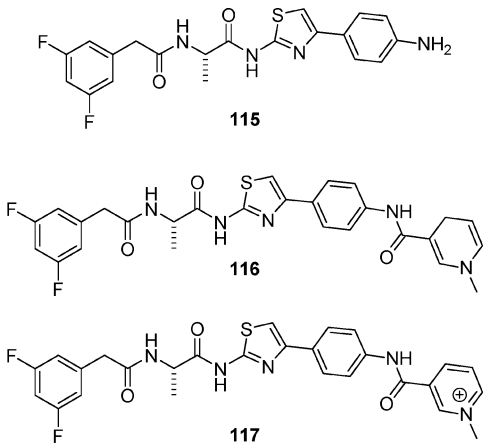

	MW	PSA (Å^2)	cLogP	cLogD	HBD	BL[a]
115	416	97	2.8	2.5	4	240
116	538	103	3.3	2.8	3	350
117	537	106	IC[b]	−1.5	3	BQL[c]

[a] Brain level (ng/g). [b] Incalculable. [c] Below the quantifiable limit.

Figure 25. Prodrug **116** improves the rate of brain uptake of **115** versus direct delivery of **115**.

Because it allows observation of the distribution of exogenous free radicals, or spin labels, electron paramagnetic resonance (EPR) operating in lower frequency bands (<1 GHz) is emerging as a useful means for imaging tissues in vivo.[73] Unfortunately, ordinary spin labels do not readily cross the BBB, which has made difficult the task of developing nitroxides for EPR brain imaging. Building on the earlier work of Yokoyama and collaborators who developed more lipophilic variants **119** and **120** of nitroxide **118**,[74] Yordanov and co-workers designed **121** and **122**, which they envisioned would be even less polar and hence more proficient at crossing the BBB (Figure 26).[73] It is important to note that masking the nitroxide functionality as a hydroxylamine ester relies on sequential transformation by esterases and oxidants in vivo to generate the active spin label (e.g., **120** → **118**).

After ip injections (500 μL of a 40 mM solution with 20% EtOH−PBS) of **121** and **122** into mice, the animals were sacrificed at 10 and 60 min time points and the concentrations of nitroxide and combined nitroxide + hydroxylamine species were measured in a number of tissues, including the brain and blood. Nitroxide concentrations in tissue were measured by EPR signal intensity, and the combined nitroxide + hydroxylamine concentrations were determined in the same manner after the tissues had been exposed to excess potassium ferricyanide to oxidize the hydroxylamine to nitroxide. Remarkably, readily detectable concentrations of both the nitroxide and hydroxylamine species derived from **121** could be measured in the brain after only 10 min (70 nmol/g), and significant concentrations persisted up to the clinically significant 60 min period (20 nmol/g). Notably, neither **122** nor the six-membered ring congener of **121** displayed useful biodistributions.

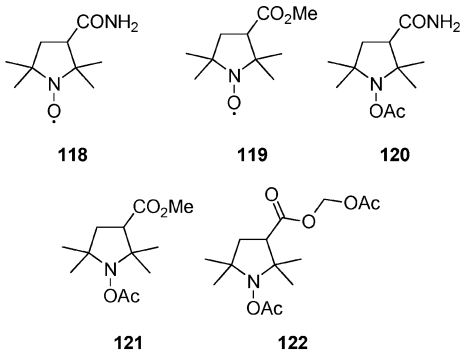

	MW	PSA (Å^2)	cLogP	cLogD	HBD	BL[a]
118	185	66	0.90	–0.65	2	ND[b]
119	200	49	2.1	0.77	0	ND[b]
120	228	73	1.7	0.15	2	ND[b]
121	243	56	2.9	1.6	0	70
122	301	82	2.8	1.7	0	NG[c]

[a] Brain level (nmol/g). [b] No data. [c] Negligible.

Figure 26. Lipophilic spin label precursor **121** readily crosses the BBB and is subsequently converted to the active nitroxide species, the polarity of which inhibits its exit from the brain.

Inhibiting Entrance

As a means to minimize the prospects for CNS-mediated side effects of drugs designed to modulate targets in the periphery, exclusion of drugs from the CNS may be preferable. A good example of such a case is the nonsedating second-generation histamine H_1 antagonists, such as 11-[*N*-(ethoxycarbonyl)-4-piperidylidene]-8-chloro-6,11-dihydro-5*H*-benzo[5,6]cyclohepta-[1,2-*b*]pyridine (loratadine), that were found retrospectively to be substrates for Pgp efflux, unlike the first-generation agents.[75] Prospectively optimizing for active efflux, however, may be a risky avenue for reducing CNS exposure and must be tempered by the knowledge that active efflux may impede absorption and/or enhance clearance in the periphery as well. Also, efflux recognition may compromise a compound's ability to access its intended biological target in some cases. This may be particularly important in oncology, where many tumor types evolve resistance through expression of efflux proteins. The case studies below illustrate a number of ways that brain penetration of drugs has been minimized.

Agonists of 5-HT_{2A} serotonin receptors have been explored as potential treatments for ocular hypertension and glaucoma. To minimize possible psychoactive side effects of brain-permeable 5-HT_{2A} agonists, Glennon and co-workers investigated incorporating polar moieties into a known agent, **123**, to decrease its lipophilicity and thereby its ability to cross the BBB (Figure 27).[76] Previous SAR studies suggested that to retain potent agonist activity, C1 of **123** was the most promising position for substitution. All possible stereoisomers of C1 methoxy- or hydroxyl-substituted congeners were investigated, but only compounds **124** and **125** displayed affinity for the 5-HT_{2A} receptor in vitro comparable to the affinity displayed by **123** (K_i = 0.50, 0.30, and 0.20 nM, respectively). Though **124** proved to be 5-fold less potent than **123** in a 5-HT_2-mediated calcium mobilization assay (EC_{50} = 0.10 vs 0.020 μM), both acted as partial agonists (efficacy of ~50%). However, by use of rat stimulus generalization as an in vivo test of CNS activity, **124** was >15 times less potent than **123**, supporting the contention that **124** does not penetrate the BBB as well as **123**.

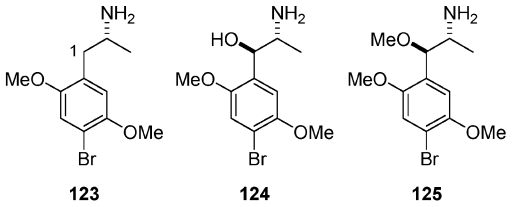

	MW	PSA (Å^2)	cLogP	cLogD	HBD	SG[a]
123	274	44	2.5	0.51	2	1
124	290	65	1.3	0.83	3	15
125	304	54	2.1	2.0	2	ND[b]

[a] Stimulus generalization (relative). [b] No data.

Figure 27. The C1-hydroxy substituent of **124** may impart decreased brain permeability compared to **123**.

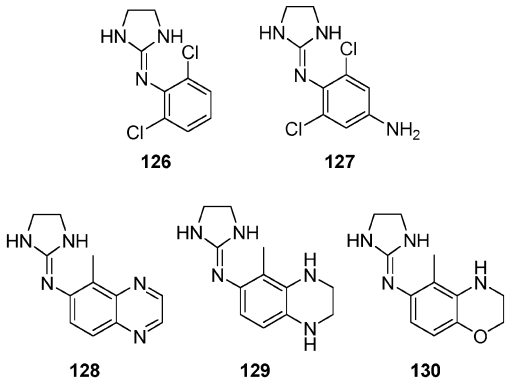

	MW	PSA (Å^2)	cLogP	cLogD	HBD	BP[a]
126	230	36	1.4	0.84	2	DDD[b]
127	245	62	0.32	–0.24	4	ND[c]
128	227	62	1.3	–2.7	2	DDD[b]
129	231	60	–0.21	–3.0	4	ND[c]
130	232	58	0.50	–2.9	3	NG[d]

[a] Blood pressure. [b] Dose-dependent decrease. [c] No data. [d] Negligible.

Figure 28. Compound **130** displays α_2 adrenoceptor agonist potency and selectivity, as well as favorable restriction from the brain.

Munk and co-workers reported some time ago their efforts to develop potent, selective, and peripherally acting α_2 adrenoceptor agonists to reduce elevated intraocular pressure (IOP).[77] Though topically administered 2,6-dichloro-*N*-(imidazolidin-2-ylidene)benzenamine (**126**, clonidine) was previously demonstrated to reduce IOP in humans, it crosses the BBB, which leads to centrally mediated side effects such as reduced blood pressure and sedation (Figure 28). The polar analogue **127** has more limited brain penetration but exhibits poor α_2/α_1 selectivity and allergy induction that may arise from its metabolic transformation into an electrophilic *p*-quinonediimide species.

Congeners **128**−**130** were designed to increase the polarity of **127** while reducing its metabolic liabilities. Though compounds **128**−**130** display respectable potency and selectivity in binding and functional assays in vitro, only **126**, **128**, and **130** lowered IOP after unilateral topical administration to rabbit eyes, and **130** did so to a greater extent than **126** (25% and 10%, respectively). Clonidine (**126**) and **128** displayed a dose-dependent decrease (DDD) in blood pressure upon peripheral administration to cynomolgus monkeys, whereas **130** did not exhibit appreciable hypotensive activity. Similar observations

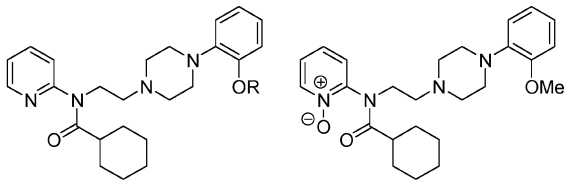

131: R = Me
132: R = H

133

	MW	PSA (Å^2)	cLogP	cLogD	HBD	MBU[a]
131	423	49	3.9	2.5[b]	0	5.0
132	409	60	3.2	2.0[b]	1	5.7
133	439	65	IC[c]	1.1[b]	0	0.54

[a] % Maximal brain uptake. [b] Ref. 78b. [c] Incalculable.

Figure 29. The *N*-oxide derivative **133** of pyridine **131** displays lower BBB permeability.

were made for **126** and **130** after iv delivery to rabbits. However, when injected directly into the fourth ventricle of the rabbit brain, **130** showed a 70% reduction in blood pressure compared to a 20% reduction for **126**. These studies, and sedation experiments in rats, buttress the assumption that **130** does not cross the BBB.

An interesting insight into the effect on BBB permeability of N-oxidation of a pyridine moiety was highlighted in a series of studies by Pike, Marchais-Oberwinkler, and co-workers directed at developing improved positron emission tomography (PET) ligands for the 5-HT$_{1A}$ receptor.[78] *N*-Pyridylamide **131** (WAY-100635) and its desmethyl analogue **132** (DWAY) are high-affinity 5-HT$_{1A}$ antagonists that have been ^{11}C-labeled to provide PET imaging tools (Figure 29). However, since **131** and **132** are rapidly cleared from plasma, there has been interest in generating potentially more stable congeners. The prophetically named analogue **133** (NOWAY), the *N*-oxide analogue of **131**, was prepared such that the amide carbonyl was labeled with ^{11}C. Compounds ^{11}C-**131** and ^{11}C-**133** were administered iv to cynomolgus monkeys, and PET was used to measure the percentage of the injected dose that reached the brain. Whereas ^{11}C-**131** showed a good maximal brain uptake (5.0%), ^{11}C-**133** exhibited a much poorer maximal brain uptake (0.54%), and consequently, in contrast to ^{11}C-**131**, it provided no ability to image 5-HT$_{1A}$ receptors in this study. By comparison of the brain uptake of **133** and **132**, the relative influence of the *N*-oxide and phenol functionalities may be evaluated. In a similar study in cynomolgus monkeys, **132** gave an excellent maximal brain uptake (5.7%), indicating that unmasking the phenolic functionality had little affect on BBB permeability when compared to **131**, in contrast to the finding with *N*-oxide **133**. The calculated log *D* (pH 7.4) values for **131**−**133** were 2.5, 2.0 and 1.1, respectively, indicating the relatively high-polarity contribution of the *N*-oxide functionality that could result in lower passive diffusion.

Other reports also indicate that *N*-oxide metabolites of brain-penetrant molecules have drastically lowered brain exposure relative to the parent pyridine and amine precursors. For example, Stöcklin and co-workers reported that 8-chloro-11-(4-methyl-1-piperazinyl)-5*H*-dibenzo[*b*,*e*][1,4]diazepine (**134**, clozapine) has a 24-fold higher brain uptake in mice after ip delivery when compared to its *N*-oxide metabolite **135** (Figure 30).[79] Another study by Baldessarini and colleagues also showed that *N*-oxide **135** does not penetrate the BBB in rat.[80] Similarly, Sveigaard et al. revealed that whereas muscarinic agonist **136** (Lu 25−109) crosses the BBB in rat (B/P = 1.0:1), its *N*-oxide

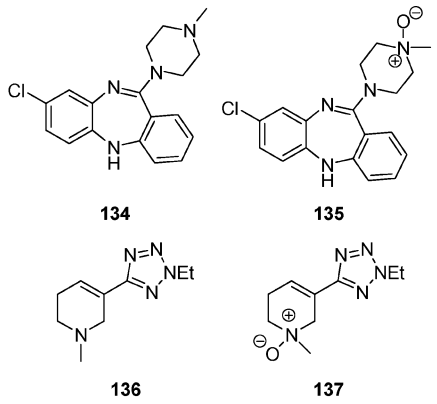

134 **135**

136 **137**

	MW	PSA (Å^2)	cLogP	cLogD	HBD	B/P
134	327	31	4.9	3.4	1	24[b]
135	343	51	IC[a]	IC[a]	1	1[b]
136	193	47	0.64	0.35[c]	0	1.0
137	209	67	IC[a]	−1.5[c]	0	NG[d]

[a] Incalculable. [b] Relative brain uptake. [c] Ref. 81. [d] Negligible.

Figure 30. Two more examples that show *N*-oxides of amines can inhibit brain penetration.

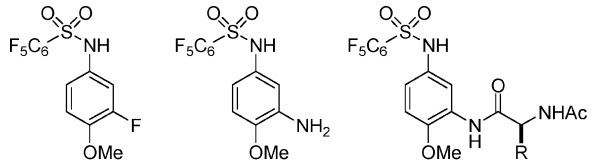

138 **139**

140: R = Me
141: R = H
142: R = CH_2OH
143: R = (*R*)-CHMeOH

	MW	PSA (Å^2)	cLogP	cLogD	HBD	BL[a]
138	371	55	3.5	2.0	1	860
139	368	81	2.6	1.2	3	1200
140	481	114	1.4	0.36	3	BQL[b]
141	467	114	1.1	0.020	3	BQL[b]
142	497	134	0.40	0.040	4	BQL[b]
143	511	134	0.71	0.39	4	12

[a] Brain level (ng/g). [b] Below the quantifiable limit.

Figure 31. Acylated derivatives **140**−**143** serve as prodrugs of **139** with limited brain permeability.

137 (Lu 32−181) does not.[81] The log *D* values of **136** and *N*-oxide **137** are 0.35 and −1.5, respectively. Generally, *N*-oxide incorporation appears to be an efficient means to limit CNS exposure.

Rubenstein and co-workers reported an interesting strategy for limiting the brain exposure of members of a class of antimitotic agents exemplified by compound **138** (T138067) (Figure 31).[82] This irreversible inhibitor of tubulin polymerization is effective against a variety of tumors, including those that express the multidrug resistant (MDR) phenotype. These investigators sought to explore less lipophilic analogues of **138** that might avoid potential CNS toxicity and thereby possess a wider therapeutic window. They hypothesized that the greater polarity of acylated congeners of aniline analogues **139** and **140**−**143** would prevent their partitioning into the brain.

Unfortunately, whereas **138** and aniline **139** displayed concentration-dependent inhibition of tubulin polymerization in vitro, amide derivatives **140**−**143** showed no significant activity.

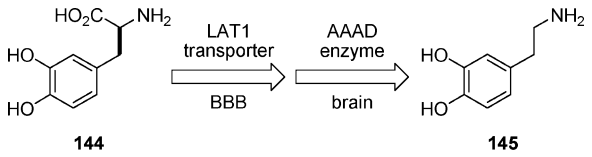

144 145

	MW	PSA (Å^2)	cLogP	cLogD	HBD
144	197	104	–2.8	–2.7	5
145	153	66	0.17	–2.0	4

Figure 32. The penetration of **144** (L-DOPA) into the brain is a classic example of the power of carrier-mediated transport across the BBB.

This lack of activity was confirmed in competition experiments: high concentrations of **138** and **139** (~5.0 μM) compete effectively with [^{3}H]-**138** (0.50 μM) for binding to purified β-tubulin (0.50 μM), but identical concentrations of **141** and **142** do not. Interestingly, amides **140**−**143** exhibited 2−7 times more potency than **138** in three cell assays for cytotoxicity (HeLa, MCF-7, and MCF-7/ADR). This apparent discrepancy is believed to arise from **140**−**143** serving as prodrugs for **139**. To support this hypothesis, glycine amide **141** was made in radiolabeled form and incubated with HepG2 cells. The half-life for [^{3}H]-**141** was ~150 min, and aniline **139** was the primary degradation product. In CD-1 mice exposed for 5 min to 30−40 mg/kg of **138**, **139**, **140**, **141**, **142**, or **143**, none of the amides except **143** showed detectable levels in the brain (12 ng/g), whereas **138** and **139** displayed much higher levels (860 and 1200 ng/g, respectively). Most importantly, aniline **139**, formed from the amides, was found in 20−5000 times lower amounts in the brain than when it was delivered directly; drastically lower plasma levels of **139** were also observed (e.g., 79-fold lower for **139** from **143**). Amide **143** (100 mg/kg iv) was able to reduce tumor size comparable to **138** by day 13 in athymic nude mice bearing MX-1 tumor xenografts.

Influencing Active Transport

Enhancing Uptake. For small molecules that possess physicochemical properties inconsistent with good BBB passive diffusion, active uptake by transport proteins is an alternative approach (Figure 1).[83] Unfortunately, few BBB transporters have been cloned and expressed to date, a problem that currently limits the scope of this strategy. Furthermore, capitalizing on an active uptake process can be capricious and poses a further challenge: in addition to binding to the target, the small molecule of interest must interact effectively with the transporter. Because they are generally quite selective, active uptake transporters often demand that for xenobiotics to be recognized, their structures should closely resemble those of the endogenous susbtrates. A favorable aspect of this approach is that a particular transporter isoform may be expressed in the endothelial cells of both the BBB and the intestinal tract, which may serve to enhance both drug absorption and brain penetration in some instances.

A classic example of the power, and potential complexity, of carrier-mediated transport is the permeation of (*S*)-2-amino-3-(3,4-dihydroxyphenyl)propanoic acid **144** (L-DOPA) into the brain by the type 1 large neutral amino acid transporter (LAT1, Figure 32).[2c] Whereas dopamine (**145**) is a water-soluble catecholamine that does not appreciably cross the BBB, **144** is actively transported across this barrier by LAT1 and then transformed by aromatic amino acid decarboxylase (AAAD) into **145**. It is critical that **144** passes both the luminal and abluminal sides of the brain capillary endothelial cells, as

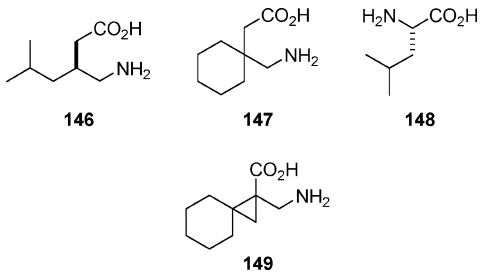

146 147 148 149

	MW	PSA (Å^2)	cLogP	cLogD	HBD	B/P
146	159	63	–0.92	–1.4	3	0.22
147	171	63	–0.66	–1.3	3	ND[a]
148	131	63	–1.7	–1.8	3	ND[a]
149	183	63	–0.81	–1.3	3	0.054

[a] No data.

Figure 33. Compounds **146**, **147**, and **149** bind to the α_2-δ subunit of voltage-gated calcium channels but have different affinities for the system L (leucine) α-amino acid transporter.

premature enzyme metabolism within these cells forms **145**, which cannot pass the abluminal membrane and partitions into the blood. This impressive prodrug delivery strategy has enabled the treatment of Parkinson's disease for several decades. The following case studies illustrate recent efforts to exploit this type of active uptake process.

Ligands for the α_2-δ subunit of voltage-gated calcium channels have been developed to modulate calcium flux at nerve terminals, aimed at attenuating neurotransmitter release to treat a variety of CNS disorders. Pregabalin (**146**) and 1-(aminomethyl)cyclohexaneacetic acid **147** (gabapentin) are known α_2-δ ligands, and **146** has displayed powerful activity in clinical and/or preclinical studies of epilepsy, anxiety, and neuropathic pain (Figure 33). Gabapentin (**147**), an anticonvulsant γ-amino acid, is transported by the system L (leucine) α-amino acid transporter, which has been proposed to account for its high accumulation gradient in brain tissue.[84] Computer modeling of **147** and L-leucine (**148**) suggests that **147**, though achiral, can assume a topography resembling the L-form of a large α-amino acid such as **148**.

While attempting to prepare analogues of **147** bearing substituents on the carbon atom α to the amino group, Schwarz and co-workers serendipitously discovered instead a route to rigid β-amino acid derivatives including **149**.[85] Though **149** showed potent binding affinity in vitro for α_2-δ (K_i = 0.013 μM), it did not display appreciable inhibitory activity against the system L transporter (IC_{50} > 2500 μM). In contrast, **146** exhibited potent binding to α_2-δ as well as good inhibitory activity against system L (K_i = 0.019 μM and IC_{50} = 160 μM). Two hours after dosing Sprague-Dawley rats with **146** or **149** (30 mg/kg po), **149** showed lower plasma (7100 ng/mL) and brain (390 ng/mL) concentrations and had a low brain-to-plasma ratio (B/P = 0.054), whereas **146** displayed significantly higher values for these measurements (19 000, 4300, and 0.22, respectively). The capacity of **146** and **147** to be transported by system L is believed to contribute significantly to these molecules entering the systemic circulation after oral dosing and permeating the blood−brain barrier. Notably, **149** exhibited anticonvulsant activity in DBA/2 mice only when injected into the cerebral ventricles (icv), whereas **146** displayed robust activity when dosed po or icv.

Subtype-selective antagonists of neuronal nicotinic acetylcholine receptors (nAChRs) have been investigated largely for

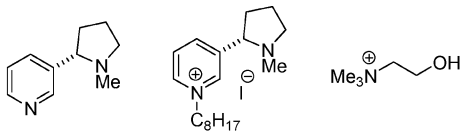

150 **151** **152**

	MW	PSA (Å^2)	cLogP	cLogD	HBD
150	162	16	0.88	0.020	0
151	275	9.1	IC[a]	–2.5	0
152	104	20	IC[a]	–3.7	1

[a] Incalculable.

Figure 34. Nicotine (**150**) is an agonist of neuronal nicotinic acetylcholine receptors (nAChRs). Its quaternary ammonium salt **151** is an antagonist that also binds to the BBB choline transporter.

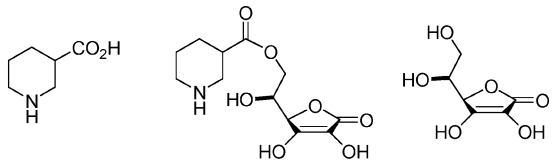

153 **154** **155**

	MW	PSA (Å^2)	cLogP	cLogD	HBD	%LC[a]
153	129	49	–2.2	–2.5	2	BQL[b]
154	287	125	–0.51	–3.1	4	50
155	176	107	–1.8	–5.3	4	ND[c]

[a] % Latency to convulsions. [b] Below the quantifiable limit. [c] No data.

Figure 35. Compound **153** does not bind with the sodium-dependent ascorbic acid transporter SVCT2. Its ascorbic acid conjugate **154** does.

use as pharmacological tools to probe the physiological roles of specific nAChR subtypes.[86] While nicotine (**150**) serves as an agonist of all known nAChR subtypes, N-quaternization of **150** transforms it into an antagonist with improved nAChR subtype selectivity (Figure 34). In theory, nAChR antagonists may be developed as potential smoking cessation agents if they can inhibit the nAChRs that mediate nicotine-induced dopamine release in the CNS. However, since these N-quaternized nicotine analogues contain a positively charged *N*-alkylpyridinium moiety, an obvious concern when considering their use as CNS drugs is that their physicochemical properties may preclude them from permeating the BBB.

Using their knowledge of structural features required for binding to the choline transporter, Crooks and collaborators have investigated extensively several such N-quaternized nicotine analogues, including *N*-*n*-octylnicotinium iodide (**151**, NONI) and congeners bearing lipophilic linear alkyl groups of different lengths.[87] In addition to **151** inhibiting the effect of nicotine on dopaminergic systems in vitro (IC_{50} = 1.1 μM), it was discovered using the in situ rat brain perfusion technique that it also binds to the BBB choline transporter (K_i = 49 μM) and enters the brain. The rate of [^{3}H]-NONI uptake can be reduced ~50% by adding either unlabeled **151** or choline (**152**) to the perfusion fluid (250 μM and 5 mM, respectively), providing further evidence that a significant component of brain uptake of **151** occurs through the BBB choline transporter. Interestingly, longer lipophilic side chains on either nicotinium or choline analogues lead to more potent BBB choline transporter affinity.

Another strategy that has been explored to increase the penetration of small molecules into the CNS is to conjugate them to endogenous compounds recognized by transporters. Glucose is an essential nutrient for the brain and known to be actively taken up by the sodium-independent GLUT1 transporter. Several laboratories have reported studies suggesting that glycosylating small molecules or peptides may facilitate permeation of those moieties across the BBB by active transport.[83] While this glucose prodrug approach is provocative, further exploration of this area is required for clearer elucidation of permeability effects and the realization of its full potential. The study detailed below is a recent attempt to use a previously unexplored nutrient−conjugate system to enhance the penetration of a small molecule into the brain.

SVCT2 is a sodium-dependent transporter known to be expressed by neuroepithelial cells of the choroid plexus and the pigmented epithelium of the retina and may serve as a portal into the brain for L-ascorbic acid (**155**) (Figure 35). Recently, Manfredini and co-workers reported their efforts toward improving the entry of small molecules into the brain by conjugating them with **155**.[88] By using human retinal pigment epithelial cells (HRPE), these workers found that the potent GABA inhibitor 3-piperidinecarboxylic acid (**153**, nipecotic acid) did not inhibit [^{14}C]ascorbic acid uptake, but its ascorbate ester **154** did (K_i = 1000 μM). Interestingly, injection of **154** (0.75 mmol/kg ip) significantly increased the latency to appearance of PTZ-induced tonic convulsions in mice, whereas **153** was ineffective at the same dose. In later studies, these workers discovered that these nipecotic acid−ascorbic acid conjugates inhibited SVCT2 to approximately the same extent irrespective of which enantiomer of **153** was used.[89] These observations contrast with those made of nonconjugated small molecules: often there is enantio- and diastereomeric discrimination by the transporters.

Mitigating Efflux. Because they are relatively promiscuous, active efflux transporters often complicate the development of treatments for CNS disorders by limiting the penetration of drugs into the brain.[90] Whereas most efflux transporters have not been well-characterized, Pgp is believed to be the most ubiquitous and is the best-characterized thus far. Therefore, several laboratories have endeavored to study the effects of Pgp on the brain penetration of their compounds both in vitro and in vivo.[9,90] An important caveat is that efflux of a given compound may result from the activity of more than one transport protein.[91] The following case studies illustrate some of the challenges Pgp efflux poses to the permeation of drugs into the brain and how those challenges have been overcome.

Audus and Georg and their co-workers recently disclosed their efforts to improve the permeation of taxoid anticancer compounds into the brain.[92] By slightly modifying the structure of paclitaxel (**156**), they hoped to reduce interactions with Pgp that are believed to contribute to its poor gastrointestinal absorption and inability to cross the BBB (Figure 36). Their plans were built upon the observation by Ojima[93] that there is a specific binding site for taxoids on Pgp and the hypothesis of Seelig[33] that there may be differences in affinity for Pgp among similar molecules with different spatial arrangements of recognition elements. After combinatorially screening dozens of analogues of **156** at C10, they discovered that a number of them retained activity in both tubulin assembly and cytotoxicity assays.[94]

Using bovine brain microvessel endothelial cells (BBMECs) and cyclosporin A (**158**) (10 μM) as the positive control for Pgp transport, these workers discovered that paclitaxel (**156**) exposure enhanced the uptake of the Pgp substrate rhodamine 123 (**159**) in a dose-dependent manner (5−25 μM), but treatment

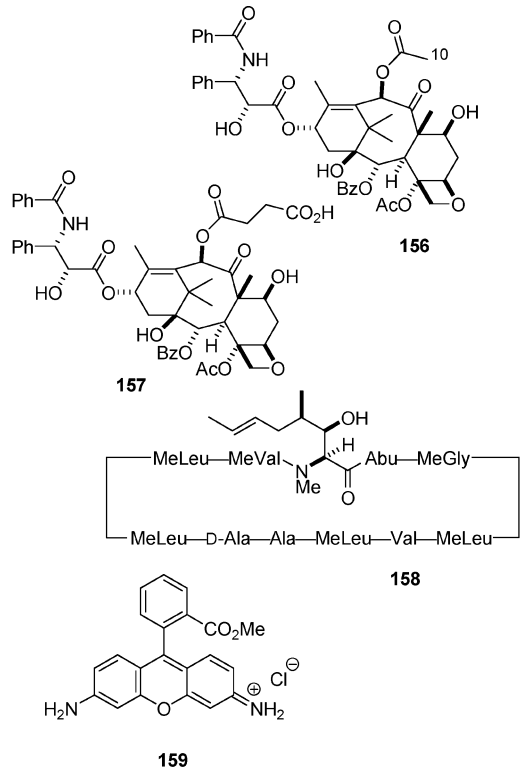

	MW	PSA (Å^2)	cLogP	cLogD	HBD	%BU[a]
156	854	221	5.0	7.2	4	2.5
157	912	259	4.7	4.0	5	6–8

[a] % Brain uptake.

Figure 36. Paclitaxel (**156**), cyclosporin A (**158**), and rhodamine 123 (**159**) are susceptible to Pgp-mediated efflux and do not partition into the brain. Derivative **157** (Tx-67) is not recognized by Pgp and crosses the BBB.

with congener **157** (25 μM) did not increase uptake of **159**. In contrast to its effect on paclitaxel (**156**) permeation, cyclosporin A (**158**) did not increase **157** penetration of BBMEC monolayers, and the permeation rates for **157** exceeded those of **156** at all concentrations examined in vitro. Employing the in situ rat brain perfusion technique, these workers found that only 2.5% of total control of **156** was detected in the brain with increasing time (30, 60, and 120 s), whereas 6−8% of **157** was retained, suggesting that it could cross the BBB. These workers also suggested that the movement of **157** through the brain capillary endothelium may be mediated by a transporter; one would expect its physicochemical properties to inhibit passive diffusion through the BBB.

Several years ago, Jimonet and co-workers reported their efforts to improve the in vivo activity of a novel series of potent antagonists of the glycine site of the NMDA receptor.[95] Such ligands are potentially useful as neuroprotective agents, as excessive stimulation of this ionotropic glutamate receptor subtype has been implicated in the neuronal death that occurs in disorders including cerebral ischemia and neurotrauma. The benzothiadiazine **160** (RPR-104632) is a potent glycine/NMDA antagonist in vitro but has only limited activity in vivo (Figure 37).[95] While the 8-chloro analogue of the novel chemotype **161** was shown to antagonize the receptor more potently than its parent (IC_{50} = 350 vs 25 nM), its poor aqueous solubility (<1 mg/mL) and potential for higher plasma protein binding were thought to be responsible for its poor activity in vivo (ED_{50} > 80 mg/kg ip).

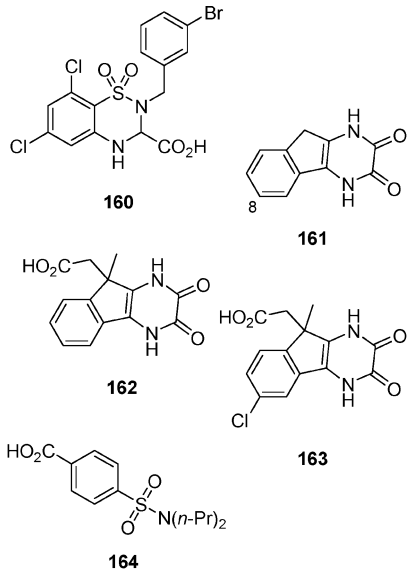

	MW	PSA (Å^2)	cLogP	cLogD	HBD	ED_{50}[a]
160	466	87	5.2	1.8	2	ND[b]
161	200	66	0.26	1.6	2	ND[b]
162	272	103	0.028	–1.3	3	65
163	307	103	0.74	–0.77	3	6.8

[a] In a mouse maximal electroshock convulsion test. [b] No data.

Figure 37. Compounds **160**−**163** are antagonists of the glycine site of the NMDA receptor, but only **163** has the sufficient balance of potency, solubility, and reduced recognition by the Na^+,K^+-ATPase active transport system to display good anticonvulsant activity in vivo.

These investigators sought to remedy these shortcomings by introducing a carboxylic acid group at a position on the scaffold **161** that could be tolerated by the binding site of the receptor.[95] Compounds **162** and **163** were found to have selective affinity for the glycine/NMDA receptor over the AMPA receptor in rat cortical membranes (IC_{50} = 21 vs 4600 and IC_{50} = 28 vs 2100 nM, respectively). Interestingly, **162** showed only weak anticonvulsant activity in the mouse maximal electroshock convulsion test (ED_{50} = 65 mg/kg ip), whereas **163** displayed more dramatic activity (ED_{50} = 6.8 mg/kg ip). Aware that the in vivo activity of several excitatory amino acid antagonists can be improved by the competitive inhibition of transport systems coupled to Na^+,K^+-ATPase, 4-[(dipropylamino)sulfonyl]benzoic acid (**164**, probenecid), the effect of co-dosing **164** with **162** and **163** was examined. While pretreatment with **164** (200 mg/kg ip) increased considerably the activity of **162** (65 → 2.7 mg/kg ip), its effect on the activity of **163** was far less dramatic (6.8 → 1.8 mg/kg ip). These results were interpreted to suggest that **163** is poorly recognized by the Na^+,K^+-ATPase transport system that may be responsible for excretion of **162** from the CNS.

Inhibitors of dihydrofolate reductase (DHFR) have demonstrated utility for the treatment of cancer and a number of infectious diseases.[96] *N*-[4-[[(2,4-Diamino-6-pteridinyl)methyl]-methylamino]benzoyl]-L-glutamic acid (**165**, methotrexate) is a hydrophilic DHFR inhibitor that has restricted distribution to the brain and depends on active transport to permeate cancer cells, a shortcoming that the more lipophilic inhibitors 5-methyl-6-[[(3,4,5-trimethoxyphenyl)amino]methyl]-2,4-quinazolinediamine (**166**, trimetrexate) and 6-[(2,5-dimethoxyphenyl)methyl]-5-methylpyrido[2,3-*d*]pyrimidine-2,4-diamine (**167**, piritrexim) do not suffer (Figure 38). However, while **166** and **167** are active against transport-impaired cells resistant to **165**, they both are

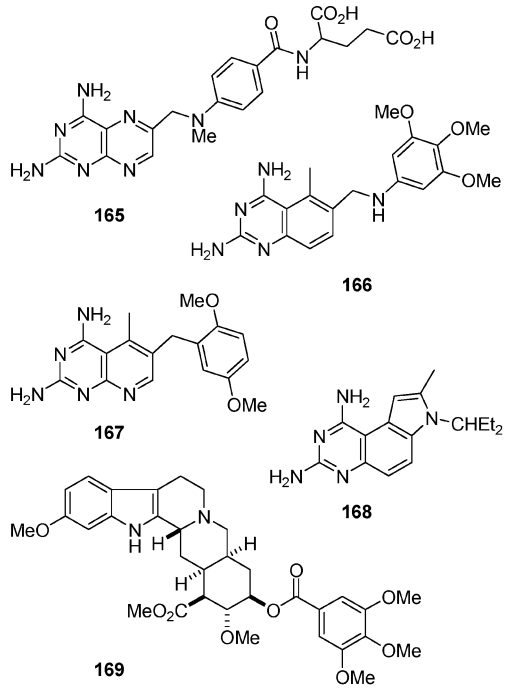

	MW	PSA (Å^2)	cLogP	cLogD	HBD	B/P
165	454	211	–0.31	–5.0	7	ND[a]
166	369	118	1.8	–1.7	5	0.10
167	325	109	2.7	1.9	4	0.65
168	283	83	4.0	2.1	4	10

[a] No data.

Figure 38. Methotrexate (**165**) is hydrophilic and relies on active transport to enter cells. Trimetrexate (**166**) and piritrexim (**167**) are lipophilic and can passively diffuse into cells but are substrates for Pgp-mediated efflux, a shortcoming that **168** does not share.

susceptible to Pgp-mediated efflux from cells expressing the multiple drug resistance phenotype (MDR) and do not distribute significantly into the brain. In 1996, Kuyper and co-workers revealed their efforts to find DHFR inhibitors with useful activity against the fungus *C. albicans* and the favorable tissue distribution profiles that **166** and **167** have but lacking Pgp susceptibility.[96] Inspired by the 7-substituted pyrrolo[3,2-*f*]quinazolines first reported by Ledig and guided by molecular modeling using the X-ray crystal structure of the holoenzyme, their investigations led to the discovery of some novel potent inhibitors, including pyrroloquinazoline **168**, with enhanced permeability.

Compound **168** exhibited potent activity against human and *C. albicans* DHFR enzymes (K_i = 0.30 and 30 pM, respectively), as well as P388D1 leukemia cell and fungus growth (IC_{50} = 0.12 nM and MIC = 0.025 μg/mL, respectively). In contrast to **166** and **167**, compound **168** was equally effective against both the parent and MDR phenotype of a number of cancer cell lines, and its cytotoxicity was not affected by reserpine (**169**), an agent that blocks the efflux activity of Pgp and can restore sensitivity of MDR cells to some anticancer drugs. In vivo experiments with CD-1 mice revealed that while **168** (60 mg/kg sc) had lower absolute plasma concentrations after 1 h (0.40 μg/mL) than **166** and **167** had after 40 min (100 and 200 mg/kg ip, respectively; 9.4 and 3.5 μg/mL, respectively), its B/P ratio of 10:1 compared favorably to those of **166** and **167** (0.10 and 0.65, respectively). Finally, **168** (12.5 mg/kg sc) was more active than **166** and **167** (4.0 and 40 mg/kg ip, respectively) against intracranially implanted P388 cells.

Conclusions

The increasing appreciation within the drug discovery community of the importance of BBB permeability is clearly reflected in the escalating frequency with which this topic is the subject of discussion in the primary medicinal chemistry literature. The examples reviewed herein hopefully serve to illustrate the sensitive nature of the influence that functional group changes can exert on BBB permeability. Not surprisingly, it is clear that certain polar functional groups including sulfonamides, sulfones, tetrazoles, amine *N*-oxides, and carboxylic acids can have particularly negative effects on BBB permeability and must be incorporated with caution, particularly when working at the limits of the suggested physiochemical boundaries for CNS-accessible chemical space. In this regard, the rules-based approaches can provide useful guidelines to improve the probability of navigating toward, or away from, BBB permeable chemical space and serve to emphasize that the cumulative effect of functionality must be considered.

A longstanding issue stems from the tendency of research groups to rely on measured whole-brain drug concentrations for compound optimization and as a precursor to initiating efficacy studies. It cannot be overstated that total drug concentration from brain tissue does not reflect free unbound drug concentration and can often be misleading. This point serves to highlight that it is highly preferable to determine pharmacodynamic or receptor occupancy readout, ideally in tandem with a pharmacokinetic measurement. The absence of a universal in vitro BBB assay to accurately and consistently predict in vivo BBB permeability remains a longstanding challenge that has unfortunately increased the burden on in vivo models.

Understanding the nature and role of BBB uptake and efflux transporters clearly remains an important and emerging area. Researchers have responded to the recognition of the significant role of Pgp-mediated efflux by more routinely assessing susceptibility in vitro cell-based assays and using the mdr1a/b KO mouse for in vivo work. Capitalizing on active uptake is now also beginning to emerge as a challenging yet viable option where passive diffusion is limiting. However, much remains to be determined with respect to the influence of other transport proteins at the BBB, and further challenges exist in dealing with extrapolating from preclinical models into humans. Potential alterations in BBB integrity in response to disease can further complicate predicted compound behavior in the human setting. A key challenge for medicinal chemists resides in deciding which data provide the most relevant information to drive structural changes aimed at optimizing or minimizing BBB permeability. However, armed with the appropriate information to drive optimization, chemistry can be a powerful tool for modulating CNS exposure.

Acknowledgment. The authors thank Drs. Yaxiong Sun, Wenyuan Qian, Xiaoyang Xia, and Vellarkad Viswanadhan for their assistance calculating the physicochemical properties of several compounds and Drs. Mark Norman and Beth Hoffman for proofreading the manuscript.

Biographies

Stephen A. Hitchcock received a B.Sc. (Honors) degree in Chemistry from Loughborough University (U.K.) in 1988 and a Ph.D. in Organic Chemistry in 1992 from the University of Nottingham (U.K.) under the tutelage of Professor Gerald Pattenden. He then joined the laboratory of Professor Samuel Danishefsky at Yale University as a NATO postdoctoral fellow. In 1994, he began work at Eli Lilly in Indianapolis, IN, as a senior chemist and was the recipient of several promotions leading to eventual appointment

as Head of Lead Optimization. Dr. Hitchcock moved to Amgen in Thousand Oaks, CA, in 2004. As Director, he is currently leading a research group focused on neuroscience and oncology targets.

Lewis D. Pennington earned a B.S. degree in Chemistry (with Highest Honors) from the University of Michigan, Ann Arbor, in 1993 under the guidance of Professor Masato Koreeda. After working for 3 years at Eli Lilly in Indianapolis, IN, he joined the laboratory of Professor Larry E. Overman at the University of California, Irvine, and received a Ph.D. in Chemistry in 2002. Following a year of work at Array BioPharma in Boulder, CO, Dr. Pennington joined Amgen in Thousand Oaks, CA, in 2003, where he is currently engaged in the investigation of agents for treating CNS disorders.

References

(1) *The Blood−Brain Barrier: Biology and Research Protocols*; Nag, S., Ed.; Methods in Molecular Medicine; Humana Press: Totowa, NJ, 2003; Vol. 89.

(2) (a) Pardridge, W. M. Transport of Small Molecules through the Blood−Brain Barrier: Biology and Methodology. *Adv. Drug Delivery Rev.* **1995**, *15*, 5−36. (b) *Introduction to the Blood−Brain Barrier: Methodology, Biology and Pathology*; Pardridge, W. M., Ed.; Cambridge University Press: New York, 1998. (c) Pardridge, W. M. Blood−Brain Barrier Drug Targeting: The Future of Brain Drug Development. *Mol. Interventions* **2003**, *3*, 90−105.

(3) (a) Aigner, A.; Wolf, S.; Gassen, G. H. Transport and Detoxification: Principles, Approaches, and Perspectives for Research on the Blood−Brain Barrier. *Angew. Chem., Int. Ed. Engl.* **1997**, *36*, 25−41. (b) El-Bacha, R. S.; Minn, A. Drug Metabolizing Enzymes in Cerebrovascular Endothelial Cells Afford a Metabolic Protection to the Brain. *Cell. Mol. Biol.* **1999**, *45*, 15−23. (c) Minn, A.; Ghersi-Egea, J.-F.; Perrin, R.; Leininger, B.; Siest, G. Drug Metabolizing Enzymes in the Brain and Cerebral Microvessels. *Brain Res. Rev.* **1991**, *16*, 65−82.

(4) de Boer, A. G.; van der Sandt, I. C. J.; Gaillard, P. J. The Role of Drug Transporters at the Blood−Brain Barrier. *Annu. Rev. Pharmacol. Toxicol.* **2003**, *43*, 629−656.

(5) Bradbury, M. W. History and Physiology of the Blood−Brain Barrier in Relation to Delivery of Drugs to the Brain. In *The Blood−Brain Barrier and Drug Delivery to the CNS*; Begley, D. J., Bradbury, M. W., Kreuter, J., Eds.; Marcel Dekker: New York, 2000; pp 1−7.

(6) (a) Clark, D. E. Computational Prediction of Blood−Brain Barrier Permeation. *Annu. Rep. Med. Chem.* **2005**, *40*, 403−415. (b) Clark, D. E. In Silico Prediction of Blood−Brain Barrier Permeation. *Drug Discovery Today* **2003**, *8*, 927−933. (c) Kaznessis, Y. N. A Review of Methods for Computational Prediction of Blood−Brain Partitioning. *Curr. Med. Chem.: Cent. Nerv. Syst. Agents* **2005**, *5*, 185−191. (d) Goodwin, J. T.; Clark, D. E. In Silico Predictions of Blood−Brain Barrier Penetration: Considerations To "Keep in Mind." *J. Pharmacol. Exp. Ther.* **2005**, *315*, 477−483. (e) Ecker, G. F.; Noe, C. R. In Silico Prediction Models for Blood−Brain Barrier Permeation. *Curr. Med. Chem.* **2004**, *11*, 1617−1628.

(7) (a) Terasaki, T.; Ohtsuki, S.; Hori, S.; Takanaga, H.; Nakashima, E.; Hosoya, K.-i. New Approaches to in Vitro Models of Blood−Brain Barrier Drug Transport. *Drug Discovery Today* **2003**, *8*, 944−954. (b) Garberg, P.; Ball, M.; Borg, N.; Cecchelli, R.; Fenart, L.; Hurst, R. D.; Lindmark, T.; Mabondzo, A.; Nilsson, J. E.; Raub, T. J.; Stanimirovic, D.; Terasaki, T.; Öberg, J.-O.; Österberg, T. In Vitro Models for the Blood−Brain Barrier. *Toxicol. in Vitro* **2005**, *19*, 299−334.

(8) (a) Abbott, N. J. Prediction of Blood−Brain Barrier Permeation in Drug Discovery from in Vivo, in Vitro and in Silico Models. *Drug Discovery Today: Technol.* **2004**, *1*, 407−416. (b) Feng, M. R. Assessment of Blood−Brain Barrier Penetration: In Silico, in Vitro and in Vivo. *Curr. Drug Metab.* **2002**, *3*, 647−657.

(9) Raub, T. J. P-Glycoprotein Recognition of Substrates and Circumvention through Rational Drug Design. *Mol. Pharm.* **2005**, *3*, 3−25.

(10) (a) Bickel, U.; Yoshikawa, T.; Pardridge, W. M. Delivery of Peptides and Proteins through the Blood−Brain Barrier. *Adv. Drug Delivery Rev.* **2001**, *46*, 247−279. (b) Prokai-Tatrai, K.; Prokai, L. Modifying Peptide Properties by Prodrug Design for Enhanced Transport into the CNS. In *Peptide Transport and Delivery into the Central Nervous System*; Prokai-Tatrai, K., Prokai, L., Eds.; Progress in Drug Research; Birkhäuser Verlag: Basel, Switzerland, 2003; pp 155−188.

(11) (a) Narayanan, R.; Gunturi, S. B. In Silico ADME Modelling: Prediction Models for Blood−Brain Barrier Permeation Using a Systematic Variable Selection Method. *Bioorg. Med. Chem.* **2005**, *13*, 3017−3028. (b) Ma, X.-l.; Chen, C.; Yang, J. Predictive Model of Blood−Brain Barrier Penetration of Organic Compounds. *Acta Pharmacol. Sin.* **2005**, *26*, 500−512. (c) Lessigiarska, I.; Pajeva, I.; Cronin, M. T. D.; Worth, A. P. 3D QSAR Investigation of the Blood−Brain Barrier Penetration of Chemical Compounds. *SAR QSAR Environ. Res.* **2005**, *16*, 79−91. (d) Winkler, D. A.; Burden, F. R. Modelling Blood−Brain Barrier Partitioning Using Bayesian Neural Nets. *J. Mol. Graphics Modell.* **2004**, *22*, 499−505. (e) Liu, X.; Tu, M.; Kelly, R. S.; Chen, C.; Smith, B. J. Development of a Computational Approach To Predict Blood−Brain Barrier Permeability. *Drug Metab. Dispos.* **2004**, *32*, 132−139.

(12) Faassen, F.; Vogel, G.; Spanings, H.; Vromans, H. Caco-2 Permeability, P-Glycoprotein Transport Ratios and Brain Penetration of Heterocyclic Drugs. *Int. J. Pharm.* **2003**, *263*, 113−122.

(13) Avdeef, A. The Rise of PAMPA. *Expert Opin. Drug Metab. Toxicol.* **2005**, *1*, 325−342.

(14) (a) Reichel, A.; Begley, D. J. Potential of Immobilized Artificial Membranes for Predicting Drug Penetration across the Blood−Brain Barrier. *Pharm. Res.* **1998**, *15*, 1270−1274. (b) Yoon, C. H.; Kim, S. J.; Shin, B. S.; Lee, K. C.; Yoo, S. D. Rapid Screening of Blood−Brain Barrier Penetration of Drugs Using the Immobilized Artificial Membrane Phosphatidylcholine Column Chromatography. *J. Biomol. Screening* **2006**, *11*, 13−20.

(15) (a) Hansen, D. K; Scott, D. O.; Otis, K. W.; Lunte, S. M. Comparison of in Vitro BBMEC Permeability and in Vivo CNS Uptake by Microdialysis Sampling. *J. Pharm. Biomed. Anal.* **2002**, *27*, 945−958. (b) Lundquist, S.; Renftel, M.; Brillault, J.; Fenart, L.; Cecchelli, R.; Dehouck, M.-P. Prediction of Drug Transport through the Blood−Brain Barrier in Vivo: A Comparison between Two in Vitro Models. *Pharm. Res.* **2002**, *19*, 976−981.

(16) Wang, Q.; Rager, J. D.; Weinstein, K.; Kardos, P. S.; Dobson, G. L.; Li, J.; Hidalgo, I. J. Evaluation of the MDR-MDCK Cell Line as a Permeability Screen for the Blood−Brain Barrier. *Int. J. Pharm.* **2005**, *288*, 349−359.

(17) Maurer, T. S.; DeBartolo, D. B.; Tess, D. A.; Scott, D. O. Relationship between Exposure and Nonspecific Binding of Thirty-Three Central Nervous System Drugs in Mice. *Drug Metab. Dispos.* **2005**, *33*, 175−181.

(18) (a) Liu, X.; Smith, B. J.; Chen, C.; Callegari, E.; Becker, S. L.; Chen, X.; Cianfrogna, J.; Doran, A. C.; Doran, S. D.; Gibbs, J. P.; Hosea, N.; Liu, J.; Nelson, F. R.; Szewc, M. A.; Van Deusen, J. Use of a Physiologically Based Pharmocokinetic Model To Study the Time To Reach Brain Equilibrium: An Experimental Analysis of the Role of Blood−Brain Barrier Permeability, Plasma Protein Binding, and Brain Tissue Binding. *J. Pharmacol. Exp. Ther.* **2005**, *313*, 1254−1262. (b) Liu, X.; Chen, C. Strategies To Optimize Brain Penetration in Drug Discovery. *Curr. Opin. Drug Discovery Dev.* **2005**, *8*, 505−512.

(19) Summerfield, S. G.; Stevens, A. J.; Cutler, L.; del Carmen, Osuna, M.; Hammond, B.; Tang, S.-P.; Hersey, A.; Spalding, D. J.; Jeffrey, P. Improving the in Vitro Prediction of in Vivo Central Nervous System Penetration: Integrating Permeability, P-glycoprotein Efflux, and Free Fractions in Blood and Brain. *J. Pharmacol. Exp. Ther.* **2006**, *316*, 1282−1290.

(20) (a) Laruelle, M.; Slifstein, M.; Huang, Y. Relationships between Radiotracer Properties and Image Quality in Molecular Imaging of the Brain with Positron Emission Tomography. *Mol. Imaging Biol.* **2003**, *5*, 363−375. (b) Waterhouse, R. N. Determination of Lipophilicity and Its Use as a Predictor of Blood−Brain Barrier Penetration of Molecular Imaging Agents. *Mol. Imaging Biol.* **2003**, *5*, 376−389.

(21) Takasato, Y.; Rapoport, S. I.; Smith, Q. R. An in Situ Brain Perfusion Technique To Study Cerebrovascular Transport in the Rat. *Am. J. Physiol.* **1984**, *247*, H484−H493.

(22) Chernet, E.; Martin, L. J.; Li, D.; Need, A. B.; Barth, V. N.; Rash, K. S.; Phebus, L. A. Use of LC/MS To Assess Brain Tracer Distribution in Preclinical, in Vivo Receptor Occupancy Studies: Dopamine D2, Serotonin 2A and NK-1 Receptors as Examples. *Life Sci.* **2005**, *78*, 340−346.

(23) Overton, E. *Vierteljahrsschr. Naturforsch. Ges. Zuerich* **1899**, *44*, 88−135.

(24) Soloway, A. H. Correlation of Drug Penetration of Brain and Chemical Structure. *Science* **1958**, *128*, 1572−1574.

(25) (a) Hansch, C.; Björkroth, J. P.; Leo, A. Hydrophobicity and Central Nervous System Agents: On the Principle of Minimal Hydrophobicity in Drug Design. *J. Pharm. Sci.* **1987**, *76*, 663−687. (b) Glave, W. R.; Hansch, C. Relationship between Lipophilic Character and Anesthetic Activity. *J. Pharm. Sci.* **1972**, *61*, 589−591.

(26) Young, R. C.; Mitchell, R. C.; Brown, T. H.; Ganellin, C. R.; Griffiths, R.; Jones, M.; Rana, K. K.; Saunders, D.; Smith, I. R.; Sore, N. E.; Wilks, T. J. Development of a New Physicochemical Model for Brain Penetration and Its Application to the Design of Centrally Acting H_2 Receptor Histamine Antagonists. *J. Med. Chem.* **1988**, *31*, 656−671.

(27) (a) Lipinski, C. A. Lead- and Drug-like Compounds: The Rule-of-Five Revolution. *Drug Discovery Today: Technol.* **2004**, *1*, 337−341. (b) Lipinski, C.; Hopkins, A. Navigating Chemical Space for Biology and Medicine. *Nature* **2004**, *432*, 855−861. (c) Lipinski, C. A. Drug-like Properties and the Causes of Poor Solubility and Poor Permeability. *J. Pharmacol. Toxicol. Methods* **2000**, *44*, 235−249.

(28) Mahar Doan, K. M.; Humphreys, J. E.; Webster, L. O.; Wring, S. A.; Shampine, L. J.; Serabjit-Singh, C. J.; Adkison, K. K.; Polli, J. W. Passive Permeability and P-Glycoprotein-Mediated Efflux Differentiate Central Nervous System (CNS) and Non-CNS Marketed Drugs. *J. Pharmacol. Exp. Ther.* **2002**, *303*, 1029−1037.

(29) (a) Begley, D. J. ABC Transporters and the Blood−Brain Barrier. *Curr. Pharm. Des.* **2004**, *10*, 1295−1312. (b) Fromm, M. F. Importance of P-Glycoprotein at Blood−Tissue Barriers. *Trends Pharmacol. Sci.* **2004**, *25*, 423−429. (c) Laplante, A.; Jodoin, J.; Demeule, M.; Béliveau, R. P-Glycoprotein: A Key Player in the Blood−Brain Barrier. *Recent Res. Dev. Biochem.* **2000**, *2*, 51−64.

(30) Kusuhara, H.; Sugiyama, Y. Active Efflux across the Blood−Brain Barrier: Role of the Solute Carrier Family. *NeuroRx* **2005**, *2*, 73−85.

(31) Schinkel, A. H.; Smit, J. J. M.; van Tellingen, O.; Beijnen, J. H.; Wagenaar, E.; van Deemter, L.; Mol, C. A. A. M.; van der Valk, M. A.; Robanus-Maandag, E. C.; te Riele, H. P. J.; Berns, A. J. M.; Borst, P. Disruption of the Mouse mdr1a P-Glycoprotein Gene Leads to a Deficiency in the Blood−Brain Barrier and to Increased Sensitivity to Drugs. *Cell* **1994**, *77*, 491−502.

(32) Doran, A.; Obach, R. S.; Smith, B. J.; Hosea, N. A.; Becker, S.; Callegari, E.; Chen, C.; Chen, X.; Choo, E.; Cianfrogna, J.; Cox, L. M.; Gibbs, J. P.; Gibbs, M. A.; Hatch, H.; Hop, C. E. C. A.; Kasman, I. N.; LaPerle, J.; Liu, J.; Liu, X.; Logman, M.; Maclin, D.; Nedza, F. M.; Nelson, F.; Olson, E.; Rahematpura, S.; Raunig, D.; Rogers, S.; Schmidt, K.; Spracklin, D. K.; Szewc, M.; Troutman, M.; Tseng, E.; Tu, M.; Van, Deusen, J. W.; Venkatakrishnan, K.; Walens, G.; Wang, E. Q.; Wong, D.; Yasgar, A. S.; Zhang, C. The Impact of P-Glycoprotein on the Disposition of Drugs Targeted for Indications of the Central Nervous System: Evaluation Using the MDR1A/1B Knockout Mouse Model. *Drug Metab. Dispos.* **2005**, *33*, 165−174.

(33) Seelig, A. How Does P-Glycoprotein Recognize Its Substrates? *Int. J. Clin. Pharmacol. Ther.* **1998**, *36*, 50−54.

(34) Abraham, M. H. The Factors That Influence Permeation across the Blood−Brain Barrier. *Eur. J. Med. Chem.* **2004**, *39*, 235−240.

(35) Gratton, J. A.; Abraham, M. H.; Bradbury, M. W.; Chadha, H. S. Molecular Factors Influencing Drug Transfer across the Blood−Brain Barrier. *J. Pharm. Pharmacol.* **1997**, *49*, 1211−1216.

(36) (a) Atkinson, F.; Cole, S.; Green, C.; van de Waterbeemd, H. Lipophilicity and Other Parameters Affecting Brain Penetration. *Curr. Med. Chem.: Cent. Nerv. Syst. Agents* **2002**, *2*, 229−240. (b) van de Waterbeemd, H.; Camenisch, G.; Folkers, G.; Chretien, J. R.; Raevsky, O. A. Estimation of Blood−Brain Barrier Crossing of Drugs Using Molecular Size and Shape, and H-Bonding Descriptors. *J. Drug Targeting* **1998**, *6*, 151−165.

(37) (a) Unless otherwise specified, all physicochemical properties in the figure tables were calculated using Advanced Chemistry Development (ACD/Labs) software (Web site: www.acdlabs.com) except for clogP values, which were obtained using Daylight Chemical Information Systems software (Web site: www.daylight.com). (b) Abbreviations employed in the figure tables: molecular weight (MW), polar surface area (PSA) in $Å^2$, calculated log *P* (cLogP), calculated log *D* (cLogD), and hydrogen bond donors (HBD).

(38) Ahmed, M.; Briggs, M. A.; Bromidge, S. M.; Buck, T.; Campbell, L.; Deeks, N. J.; Garner, A.; Gordon, L.; Hamprecht, D. W.; Holland, V.; Johnson, C. N.; Medhurst, A. D.; Mitchell, D. J.; Moss, S. F.; Powles, J.; Seal, J. T.; Stean, T. O.; Stemp, G.; Thompson, M.; Trail, B.; Upton, N.; Winborn, K.; Witty, D. R. Bicyclic Heteroarylpiperazines as Selective Brain Penetrant 5-HT_6 Receptor Antagonists. *Bioorg. Med. Chem. Lett.* **2005**, *15*, 4867−4871.

(39) (a) Tatsumi, R.; Fujio, M.; Satoh, H.; Katayama, J.; Takanashi, S.-i.; Hashimoto, K.; Tanaka, H. Discovery of the a7 Nicotinic Acetylcholine Receptor Agonists. (*R*)-3′-(5-Chlorothiophen-2-yl)-spiro-1-azabicyclo[2.2.2]octane-3,5′-[1′,3′]oxazolidin-2′-one as a Novel, Potent, Selective, and Orally Bioavailable Ligand. *J. Med. Chem.* **2005**, *48*, 2678−2686. (b) Tatsumi, R.; Seio, K.; Fujio, M.; Katayama, J.; Horikawa, T.; Hashimoto, K.; Tanaka, H. (+)-3-[2-(Benzo[*b*]-thiophen-2-yl)-2-oxoethyl]-1-azabicyclo[2.2.2]octane as Potent Agonists for the α7 Nicotinic Acetylcholine Receptor. *Bioorg. Med. Chem. Lett.* **2004**, *14*, 3781−3784.

(40) Campiani, G.; Morelli, E.; Gemma, S.; Nacci, V.; Butini, S.; Hamon, M.; Novellino, E.; Greco, G.; Cagnotto, A.; Goegan, M.; Cervo, L.; Valle, F. D.; Fracasso, C.; Caccia, S.; Mennini, T. Pyrroloquinoxaline Derivatives as High-Affinity and Selective 5-HT_3 Receptor Agonists: Synthesis, Further Structure−Activity Relationships, and Biological Studies. *J. Med. Chem.* **1999**, *42*, 4362−4379.

(41) Campiani, G.; Cappelli, A.; Nacci, V.; Anzini, M.; Vomero, S.; Hamon, M.; Cagnotto, A.; Fracasso, C.; Uboldi, C.; Caccia, S.; Consolo, S.; Mennini, T. Novel and Highly Potent 5-HT_3 Receptor Agonists Based on a Pyrroloquinoxaline Structure. *J. Med. Chem.* **1997**, *40*, 3670−3678.

(42) Habgood, M. D.; Liu, Z. D.; Dehkordi, L. S.; Khodr, H. H.; Abbott, J.; Hider, R. C. Investigation into the Correlation between the Structure of Hydroxypyridinones and Blood−Brain Barrier Permeability. *Biochem. Pharmacol.* **1999**, *57*, 1305−1310.

(43) Boyd, H. F.; Hammond, B.; Hickey, D. M. B.; Ife, R. J.; Leach, C. A.; Lewis, V. A.; Macphee, C. H.; Milliner, K. J.; Pinto, I. L.; Smith, S. A.; Stansfield, I. G.; Theobald, C. J.; Whittaker, C. M. The Identification of a Potent, Water Soluble Inhibitor of Lipoprotein-Associated Phospholipase A_2. *Bioorg. Med. Chem. Lett.* **2001**, *11*, 701−704.

(44) Boyd, H. F.; Fell, S. C. M.; Flynn, S. T.; Hickey, D. M. B.; Ife, R. J.; Leach, C. A.; Macphee, C. H.; Milliner, K. J.; Moores, K. E.; Pinto, I. L.; Porter, R. A.; Rawlings, A. D.; Smith, S. A.; Stansfield, I. G.; Tew, D. G.; Theobald, C. J.; Whittaker, C. M. N-1 Substituted Pyrimidin-4-ones: Novel, Orally Active Inhibitors of Lipoprotein-Associated Phospholipase A_2. *Bioorg. Med. Chem. Lett.* **2000**, *10*, 2557−2561.

(45) Xu, Y.; Choi, S.-R.; Kung, M.-P.; Kung, H. F. Synthesis of Radioiodinated 1-Deoxy-Nojirimycin Derivatives: Novel Glucose Analogs. *Nucl. Med. Biol.* **1999**, *26*, 833−839.

(46) Zhuang, Z.-P.; Kung, M.-P.; Hou, C.; Skovronsky, D. M.; Gur, T. L.; Plössl, K.; Trojanowski, J. Q.; Lee, V. M.-Y.; Kung, H. F. Radioiodinated Styrylbenzenes and Thioflavins as Probes for Amyloid Aggregates. *J. Med. Chem.* **2001**, *44*, 1905−1914.

(47) Sakurai, T.; Amemiya, A.; Ishii, M.; Matsuzaki, I.; Chemelli, R. M.; Tanaka, H.; Williams, S. C.; Richardson, J. A.; Kozlowski, G. P.; Wilson, S.; Arch, J. R. S.; Buckingham, R. E.; Haynes, A. C.; Carr, S. A.; Annan, R. S.; McNulty, D. E.; Liu, W.-S.; Terrett, J. A.; Elshourbagy, N. A.; Bergsma, D. J.; Yanagisawa, M. Orexins and Orexin Receptors: A Family of Hypothalamic Neuropeptides and G Protein-Coupled Receptors That Regulate Feeding Behavior. *Cell* **1998**, *92*, 573−585.

(48) Porter, R. A.; Chan, W. N.; Coulton, S.; Johns, A.; Hadley, M. S.; Widdowson, K.; Jerman, J. J. C.; Brough, S. J.; Coldwell, M.; Smart, D.; Jewitt, F.; Jeffrey, P.; Austin, N. 1,3-Biarylureas as Selective Non-Peptide Antagonists of the Orexin-1 Receptor. *Bioorg. Med. Chem. Lett.* **2001**, *11*, 1907−1910.

(49) Stemp, G.; Ashmeade, T.; Branch, C. L.; Hadley, M. S.; Hunter, A. J.; Johnson, C. N.; Nash, D. J.; Thewlis, K. M.; Vong, A. K. K.; Austin, N. E.; Jeffrey, P.; Avenell, K. Y.; Boyfield, I.; Hagan, J. J.; Middlemiss, D. N.; Reavill, C.; Riley, G. J.; Routledge, C.; Wood, M. Design and Synthesis of *trans*-*N*-[4-[2-(6-Cyano-1,2,3,4-tetrahydroisoquinolin-2-yl)ethyl]cyclohexyl]-4-quinolinecarboxamide (SB-277011): A Potent and Selective Dopamine D_3 Receptor Antagonist with High Oral Bioavailability and CNS Penetration in the Rat. *J. Med. Chem.* **2000**, *43*, 1878−1885.

(50) Vasudevan, A.; Souers, A. J.; Freeman, J. C.; Verzal, M. D.; Gao, J.; Mulhern, M. M.; Wodka, D.; Lynch, J. K.; Engstrom, K. M.; Wagaw, S. H.; Brodjian, S.; Dayton, B.; Falls, D. H.; Bush, E.; Brune, M.; Shapiro, R. D.; Marsh, K. C.; Hernandez, L. E.; Collins, C. A.; Kym, P. R. Aminopiperidine Indazoles as Orally Efficacious Melanin Concentrating Hormone Receptor-1 Antagonists. *Bioorg. Med. Chem. Lett.* **2005**, *15*, 5293−5297.

(51) (a) Bromidge, S. M.; Clarke, S. E.; King, F. D.; Lovell, P. J.; Newman, H.; Riley, G.; Routledge, C.; Serafinowska, H. T.; Smith, D. R.; Thomas, D. R. Bicyclic Piperazinylbenzenesulphonamides Are Potent and Selective 5-HT_6 Receptor Antagonists. *Bioorg. Med. Chem. Lett.* **2002**, *12*, 1357−1360. (b) Bromidge, S. M.; Brown, A. M.; Clarke, S. E.; Dodgson, K.; Gager, T.; Grassam, H. L.; Jeffrey, P. M.; Joiner, G. F.; King, F. D.; Middlemiss, D. N.; Moss, S. F.; Newman, H.; Riley, G.; Routledge, C.; Wyman, P. 5-Chloro-*N*-(4-methoxy-3-piperazin-1-ylphenyl)-3-methyl-2-benzothiophenesulfonamide (SB-271046): A Potent, Selective, and Orally Bioavailable 5-HT_6 Receptor Antagonist. *J. Med. Chem.* **1999**, *42*, 202−205.

(52) Fura, A.; Shu, Y.-Z.; Zhu, M.; Hanson, R. L.; Roongta, V.; Humphreys, W. G. Discovering Drugs through Biological Transformation: Role of Pharmacologically Active Metabolites in Drug Discovery. *J. Med. Chem.* **2004**, *47*, 4339−4351.

(53) Hughes, J.; Boden, P.; Costall, B.; Domeney, A.; Kelly, E.; Horwell, D. C.; Hunter, J. C.; Pinnock, R. D.; Woodruff, G. N. Development of a Class of Selective Cholecystokinin Type B Receptor Antagonists Having Potent Anxiolytic Activity. *Proc. Natl. Acad. Sci. U.S.A.* **1990**, *87*, 6728−6732.

(54) Trivedi, B. K.; Padia, J. K.; Holmes, A.; Rose, S.; Wright, D. S.; Hinton, J. P.; Pritchard, M. C.; Eden, J. M.; Kneen, C.; Webdale, L.; Suman-Chauhan, N.; Boden, P.; Singh, L.; Field, M. J.; Hill, D.

Second Generation "Peptoid" CCK-B Receptor Antagonists: Identification and Development of *N*-(Adamantyloxycarbonyl)-α-methyl-(*R*)-tryptophan Derivative (CI-1015) with an Improved Pharmacokinetic Profile. *J. Med. Chem.* **1998**, *41*, 38−45.

(55) Castro, J. L.; Ball, R. G.; Broughton, H. B.; Russell, M. G. N.; Rathbone, D.; Watt, A. P.; Baker, R.; Chapman, K. L.; Fletcher, A. E.; Patel, S.; Smith, A. J.; Marshall, G. R.; Ryecroft, W.; Matassa, V. G. Controlled Modification of Acidity in Cholecystokinin B Receptor Antagonists: *N*-(1,4-Benzodiazepin-3-yl)-*N*′-[3-(tetrazol-5-ylamino)phenyl]ureas. J. *Med. Chem.* **1996**, *39*, 842−849.

(56) Pinkerton, A. B.; Cube, R. V.; Hutchinson, J. H.; James, J. K.; Gardner, M. F.; Schaffhauser, H.; Rowe, B. A.; Daggett, L. P.; Vernier, J.-M. Allosteric Potentiators of the Metabotropic Glutamate Receptor 2 (mGlu2). Part 2: 4-Thiopyridyl Acetophenones as Non-Tetrazole Containing mGlu2 Receptor Potentiators. *Bioorg. Med. Chem. Lett.* **2004**, *14*, 5867−5872.

(57) Bonnefous, C.; Vernier, J.-M.; Hutchinson, J. H.; Gardner, M. F.; Cramer, M.; James, J. K.; Rowe, B. A.; Daggett, L. P.; Schaffhauser, H.; Kamenecka, T. M. Biphenyl-Indanones: Allosteric Potentiators of the Metabotropic Glutamate Subtype 2 Receptor. *Bioorg. Med. Chem. Lett.* **2005**, *15*, 4354−4358.

(58) Govek, S. P.; Bonnefous, C.; Hutchinson, J. H.; Kamenecka, T.; McQuiston, J.; Pracitto, R.; Zhao, L. X.; Gardner, M. F.; James, J. K.; Daggett, L. P.; Rowe, B. A.; Schaffhauser, H.; Bristow, L. J.; Campbell, U. C.; Rodriguez, D. E.; Vernier, J.-M. Benzazoles as Allosteric Potentiators of Metabotropic Glutamate Receptor 2 (mGluR2): Efficacy in an Animal Model for Schizophrenia. *Bioorg. Med. Chem. Lett.* **2005**, *15*, 4068−4072.

(59) Cube, R. V.; Vernier, J.-M.; Hutchinson, J. H.; Gardner, M. F.; James, J. K.; Rowe, B. A.; Schaffhauser, H.; Daggett, L.; Pinkerton, A. B. 3-(2-Ethoxy-4-{4-[3-hydroxy-2-methyl-4-(3-methylbutanoyl)phenoxy]-butoxy}phenyl)propanoic Acid: A Brain Penetrant Allosteric Potentiator at the Metabotropic Glutamate Receptor 2 (mGluR2). *Bioorg. Med. Chem. Lett.* **2005**, *15*, 2389−2393.

(60) (a) Eriksen, J. L.; Sagi, S. A.; Smith, T. E.; Weggen, S.; Das, P.; McLendon, D. C.; Ozols, V. V.; Jessing, K. W.; Zavitz, K. H.; Koo, E. H.; Golde, T. E. NSAIDs and Enantiomers of Flurbiprofen Target γ-Secretase and Lower Aβ_{42} in Vivo. *J. Clin. Invest.* **2003**, *112*, 440−449. (b) Yan, Q.; Zhang, J.; Liu, H.; Babu-Khan, S.; Vassar, R.; Biere, A. L.; Citron, M.; Landreth, G. Anti-Inflammatory Drug Therapy Alters β-Amyloid Processing and Deposition in an Animal Model of Alzheimer's Disease. *J. Neurosci.* **2003**, *23*, 7504−7509.

(61) Lleó, A.; Berezovska, O.; Herl, L.; Raju, S.; Deng, A.; Bacskai, B. J.; Frosch, M. P.; Irizarry, M.; Hyman, B. T. Nonsteroidal Anti-Inflammatory Drugs Lower Aβ_{42} and Change Presenilin 1 Conformation. *Nat. Med.* **2004**, *10*, 1065−1066.

(62) Peretto, I.; Radaelli, S.; Parini, C.; Zandi, M.; Raveglia, L. F.; Dondio, G.; Fontanella, L.; Misiano, P.; Bigogno, C.; Rizzi, A.; Riccardi, B.; Biscaioli, M.; Marchetti, S.; Puccini, P.; Catinella, S.; Rondelli, I.; Cenacchi, V.; Bolzoni, T. T.; Caruso, P.; Villetti, G.; Facchinetti, F.; Del Giudice, E.; Moretto, N.; Imbimbo, B. P. Synthesis and Biological Activity of Flurbiprofen Analogues as Selective Inhibitors of β-Amyloid$_{1-42}$ Secretion. *J. Med. Chem.* **2005**, *48*, 5705−5720.

(63) Kuroda, S.; Takamura, F.; Tenda, Y.; Itani, H.; Tomishima, Y.; Akahane, A.; Sakane, K. Design, Synthesis and Biological Evaluation of a Novel Series of Potent, Orally Active Adenosine A_1 Receptor Antagonists with High Blood−Brain Barrier Permeability. *Chem. Pharm. Bull.* **2001**, *49*, 988−998.

(64) (a) Hewawasam, P.; Gribkoff, V. K.; Pendri, Y.; Dworetzky, S. I.; Meanwell, N. A.; Martinez, E.; Boissard, C. G.; Post-Munson, D. J.; Trojnacki, J. T.; Yeleswaram, K.; Pajor, L. M.; Knipe, J.; Gao, Q.; Perrone, R.; Starrett, J. E. The Synthesis and Characterization of BMS-204352 (MaxiPost) and Related 3-Fluorooxindoles as Openers of Maxi-K Potassium Channels. *Bioorg. Med. Chem. Lett.* **2002**, *12*, 1023−1026. (b) Hewawasam, P.; Fan, W.; Knipe, J.; Moon, S. L.; Boissard, C. G.; Gribkoff, V. K.; Starrett, J. E. The Synthesis and Structure−Activity Relationships of 4-Aryl-3-aminoquinolin-2-ones: A New Class of Calcium-Dependent, Large Conductance, Potassium (Maxi-K) Channel Openers Targeted for Post-Stroke Neuroprotection. *Bioorg. Med. Chem. Lett.* **2002**, *12*, 1779−1783.

(65) Anderson, B. D. Prodrugs for Improved CNS Delivery. *Adv. Drug Delivery Rev.* **1996**, *19*, 171−202.

(66) Deguchi, Y.; Hayashi, H.; Fujii, S.; Naito, T.; Yokoyama, Y.; Yamada, S.; Kimura, R. Improved Brain Delivery of a Nonsteroidal Anti-Inflammatory Drug with a Synthetic Glyceride Ester: A Preliminary Attempt at a CNS Drug Delivery System for the Therapy of Alzheimer's Disease. *J. Drug Targeting* **2000**, *8*, 371−381.

(67) Kotra, L. P.; Manouilov, K. K.; Cretton-Scott, E.; Sommadossi, J.-P.; Boudinot, F. D.; Schinazi, R. F.; Chu, C. K. Synthesis, Biotransformation, and Pharmacokinetic Studies of 9-(β-D-Arabinofuranosyl)-6-azidopurine: A Prodrug for Ara-A Designed To Utilize the Azide Reduction Pathway. *J. Med. Chem.* **1996**, *39*, 5202−5207.

(68) (a) Koudriakova, T.; Manouilov, K. K.; Shanmuganathan, K.; Kotra, L. P.; Boudinot, F. D.; Cretton-Scott, E.; Sommadossi, J.-P.; Schinazi, R. F.; Chu, C. K. In Vitro and in Vivo Evaluation of 6-Azido-2′,3′-dideoxy-2′-fluoro-β-D-arabinofuranosylpurine and N^6-Methyl-2′,3′-dideoxy-2′-fluoro-β-D-arabinofuranosyladenine as Prodrugs of the Anti-HIV Nucleosides 2′-F-ara-ddA and 2′-F-ara-ddI. *J. Med. Chem.* **1996**, *39*, 4676−4681. (b) Shanmuganathan, K.; Koudriakova, T.; Nampalli, S.; Du, J.; Gallo, J. M.; Schinazi, R. F.; Chu, C. K. Enhanced Brain Delivery of an Anti-HIV Nucleoside 2′-F-ara-ddI by Xanthine Oxidase Mediated Biotransformation. *J. Med. Chem.* **1994**, *37*, 821−827.

(69) Prokai, L.; Prokai-Tatrai, K.; Bodor, N. Targeting Drugs to the Brain by Redox Chemical Delivery Systems. *Med. Res. Rev.* **2000**, *20*, 367−416.

(70) Yiu, S.-h.; Knaus, E. E. Synthesis, Biological Evaluation, Calcium Channel Antagonist Activity, and Anticonvulsant Activity of Felodipine Coupled to a Dihydropyridine−Pyridinium Salt Redox Chemical Delivery System. *J. Med. Chem.* **1996**, *39*, 4576−4582.

(71) Kimberly, W. T.; Esler, W. P.; Ye, W.; Ostaszewski, B. L.; Gao, J.; Diehl, T.; Selkoe, D. J.; Wolfe, M. S. Notch and the Amyloid Precursor Protein Are Cleaved by Similar γ-Secretase(s). *Biochemistry* **2003**, *42*, 137−144.

(72) Laras, Y.; Quéléver, G.; Garino, C.; Pietrancosta, N.; Sheha, M.; Bihel, F.; Wolfe, M. S.; Kraus, J.-L. Substituted Thiazolamide Coupled to a Redox Delivery System: A New γ-Secretase Inhibitor with Enhanced Pharmacokinetic Profile. *Org. Biomol. Chem.* **2005**, *3*, 612−618.

(73) Yordanov, A. T.; Yamada, K.-i.; Krishna, M. C.; Russo, A.; Yoo, J.; English, S.; Mitchell, J. B.; Brechbiel, M. W. Acyl-Protected Hydroxylamines as Spin Label Generators for EPR Brain Imaging. *J. Med. Chem.* **2002**, *45*, 2283−2288.

(74) (a) Yokoyama, H.; Itoh, O.; Aoyama, M.; Obara, H.; Ohya, H.; Kamada, H. In Vivo EPR Imaging by Using an Acyl-Protected Hydroxylamine To Analyze Intracerebral Oxidative Stress in Rats after Epileptic Seizures. *Magn. Reson. Imaging* **2000**, *18*, 875−879. (b) Yokoyama, H.; Itoh, O.; Ogata, T.; Obara, H.; Ohya-Nishiguchi, H.; Kamada, H. Temporal Brain Imaging by a Rapid Scan ESR-CT System in Rats Receiving Intraperitoneal Injection of a Methyl Ester Nitroxide Radical. *Magn. Reson. Imaging* **1997**, *15*, 1079−1984. (c) Yokoyama, H.; Ogata, T.; Tsuchihashi, N.; Hiramatsu, M.; Mori, N. A Spatiotemporal Study on the Distribution of Intraperitoneally Injected Nitroxide Radical in the Rat Head Using an in Vivo ESR Imaging System. *Magn. Reson. Imaging* **1996**, *14*, 559−563.

(75) Chen, C.; Hanson, H.; Watson, J. W; Lee, J. S. P-Glycoprotein Limits the Brain Penetration of Nonsedating but not Sedating H1-Antagonists. *Drug Metab. Dispos.* **2003**, *31*, 312−318.

(76) Glennon, R. A.; Bondarev, M. L.; Khorana, N.; Young, R. β-Oxygenated Analogues of the 5-HT_{2A} Serotonin Receptor Agonist 1-(4-Bromo-2,5-dimethoxyphenyl)-2-aminopropane. *J. Med. Chem.* **2004**, *47*, 6034−6041.

(77) Munk, S. A.; Harcourt, D.; Ambrus, G.; Denys, L.; Gluchowski, C.; Burke, J. A.; Kharlamb, A. B.; Manlapaz, C. A.; Padillo, E. U.; Runde, E.; Williams, L.; Wheeler, L. A.; Garst, M. E. Synthesis and Evaluation of 2-[(5-Methylbenz-1-ox-4-azin-6-yl)imino]imidazoline, a Potent, Peripherally Acting α_2 Adrenoceptor Agonist. *J. Med. Chem.* **1996**, *39*, 3533−3538.

(78) (a) Pike, V. W.; Halldin, C.; McCarron, J. A.; Lundkvist, C.; Hirani, E.; Olsson, H.; Hume, S. P.; Karlsson, P.; Osman, S.; Swahn, C.-G.; Hall, H.; Wikström, H.; Mensonidas, M.; Poole, K. G.; Farde, L. [Carbonyl-^{11}C]desmethyl-WAY-100635 (DWAY) Is a Potent and Selective Radioligand for Central 5-HT_{1A} Receptors in Vitro and in Vivo. *Eur. J. Nucl. Med.* **1998**, *25*, 338−346. (b) Marchais-Oberwinkler, S.; Nowicki, B.; Pike, V. W.; Halldin, C.; Sandell, J.; Chou, Y.-H.; Gulyas, B.; Brennum, L. T.; Farde, L.; Wikström, H. V. *N*-Oxide Analogs of WAY-100635: New High Affinity 5-HT_{1A} Receptor Antagonists. *Bioorg. Med. Chem.* **2005**, *13*, 883−893.

(79) Bender, D.; Holschbach, M.; Stöcklin, G. Synthesis of n.c.a Carbon-11 Labelled Clozapine and Its Major Metabolite Clozapine-*N*-Oxide and Comparison of Their Biodistribution in Mice. *Nucl. Med. Biol.* **1994**, *21*, 921−925.

(80) Baldessarini, R. J.; Centorrino, F.; Flood, J. G.; Volpicelli, S. A.; Huston-Lyons, D.; Cohen, B. M. Tissue Concentrations of Clozapine and Its Metabolites in the Rat. *Neuropsychopharmacology* **1993**, *9*, 117−124.

(81) Sveigaard, H. H.; Dalgaard, L. Evaluation of Blood−Brain Barrier Passage of a Muscarine M1 Agonist and a Series of Analogous Tetrahydropyridines Measured by in Vivo Microdialysis. *Pharm. Res.* **2000**, *17*, 70−76.

(82) Rubenstein, S. M.; Baichwal, V.; Beckmann, H.; Clark, D. L.; Frankmoelle, W.; Roche, D.; Santha, E.; Schwender, S.; Thoolen, M.; Ye, Q.; Jaen, J. C. Hydrophilic, Pro-Drug Analogues of T138067 Are Efficacious in Controlling Tumor Growth in Vivo and Show a Decreased Ability To Cross the Blood Brain Barrier. *J. Med. Chem.* **2001**, *44*, 3599−3605.

(83) (a) Tsuji, A. Small Molecular Drug Transfer Across the Blood−Brain Barrier via Carrier-Mediated Transport Systems. *NeuroRx* **2005**, *2*, 54−62. (b) Sai, Y.; Tsuji, A. Transporter-Mediated Drug Delivery: Recent Progress and Experimental Approaches. *Drug Discovery Today* **2004**, *9*, 712−720. (c) Tamai, I.; Tsuji, A. Transporter-Mediated Permeation of Drugs across the Blood−Brain Barrier. *J. Pharm. Sci.* **2000**, *89*, 1371−1388. (d) Tsuji, A.; Tamai, I. Carrier-Mediated or Specialized Transport of Drugs across the Blood−Brain Barrier. *Adv. Drug Delivery Rev.* **1999**, *36*, 277−290.

(84) Su, T.-Z.; Lunney, E.; Campbell, G.; Oxender, D. L. Transport of Gabapentin, a γ-Amino Acid Drug, by System L α-Amino Acid Transporters: A Comparative Study in Astrocytes, Synaptosomes, and CHO Cells. *J. Neurochem.* **1995**, *64*, 2125−2131.

(85) Schwarz, J. B.; Gibbons, S. E.; Graham, S. R.; Colbry, N. L.; Guzzo, P. R.; Le, V.-D.; Vartanian, M. G.; Kinsora, J. J.; Lotarski, S. M.; Li, Z.; Dickerson, M. R.; Su, T.-Z.; Weber, M. L.; El-Kattan, A.; Thorpe, A. J.; Donevan, S. D.; Taylor, C. P.; Wustrow, D. J. Novel Cyclopropyl β-Amino Acid Analogues of Pregabalin and Gabapentin That Target the α_2-d Protein. *J. Med. Chem.* **2005**, *48*, 3026−3035.

(86) Crooks, P. A.; Ayers, J. T.; Xu, R.; Sumithran, S. P.; Grinevich, V. P.; Wilkins, L. H.; Deaciuc, A. G.; Allen, D. D.; Dwoskin, L. P. Development of Subtype-Selective Ligands as Antagonists at Nicotinic Receptors Mediating Nicotine-Evoked Dopamine Release. *Bioorg. Med. Chem. Lett.* **2004**, *14*, 1869−1874.

(87) Allen, D. D.; Lockman, P. R.; Roder, K. E.; Dwoskin, L. P.; Crooks, P. A. Active Transport of High-Affinity Choline and Nicotine Analogs into the Central Nervous System by the Blood−Brain Barrier Choline Transporter. *J. Pharmacol. Exp. Ther.* **2003**, *304*, 1268−1274.

(88) Manfredini, S.; Pavan, B.; Vertuani, S.; Scaglianti, M.; Compagnone, D.; Biondi, C.; Scatturin, A.; Tanganelli, S.; Ferraro, L.; Prasad, P.; Dalpiaz, A. Design, Synthesis and Activity of Ascorbic Acid Prodrugs of Nipecotic, Kynurenic and Diclophenamic Acids, Liable To Increase Neurotropic Activity. *J. Med. Chem.* **2002**, *45*, 559−562.

(89) Manfredini, S.; Vertuani, S.; Pavan, B.; Vitali, F.; Scaglianti, M.; Bortolotti, F.; Biondi, C.; Scatturin, A.; Prasad, P.; Dalpiaz, A. Design, Synthesis and in Vitro Evaluation on HRPE Cells of Ascorbic and 6-Bromoascorbic Acid Conjugates with Neuroactive Molecules. *Bioorg. Med. Chem.* **2004**, *12*, 5453−5463.

(90) (a) Löscher, W.; Potschka, H. Blood−Brain Barrier Active Efflux Transporters: ATP-Binding Cassette Gene Family. *NeuroRx* **2005**, *2*, 86−98. (b) Löscher, W.; Potschka, H. Role of Drug Efflux Transporters in the Brain for Drug Disposition and Treatment of Brain Diseases. *Prog. Neurobiol.* **2005**, *76*, 22−76. (c) El Ela, A. A.; Härtter, S.; Schmitt, U.; Hiemke, C.; Spahn-Langguth, H.; Langguth, P. Identification of P-Glycoprotein Substrates and Inhibitors among Psychoactive Compounds. Implications for Pharmacokinetics of Selected Substrates. *Pharm. Pharmacol.* **2004**, *56*, 967−975. (d) Golden, P. L.; Pollack, G. M. Blood−Brain Barrier Efflux Transport. *J. Pharm. Sci.* **2003**, *92*, 1739−1753. (e) Seelig, A.; Landwojtowicz, E. Structure−Activity Relationship of P-Glycoprotein Substrates and Modifiers. *Eur. J. Pharm. Sci.* **2000**, *12*, 31−40.

(91) Murata, M.; Tamai, I.; Kato, H.; Nagata, O.; Kato, H.; Tsuji, A. Efflux Transport of a New Quinolone Antibacterial Agent, HSR-903, across the Blood−Brain Barrier. *J. Pharmacol. Exp. Ther.* **1999**, *290*, 51−57.

(92) Rice, A.; Liu, Y.; Michaelis, M. L.; Himes, R. H.; Georg, G. I.; Audus, K. L. Chemical Modification of Paclitaxel (Taxol) Reduces P-Glycoprotein Interactions and Increases Permeation across the Blood−Brain Barrier in Vitro and in Situ. *J. Med. Chem.* **2005**, *48*, 832−838.

(93) Ojima, I.; Duclos, O.; Dormán, G.; Simonot, B.; Prestwich, G. D.; Rao, S.; Lerro, K. A.; Horwitz, S. B. A New Paclitaxel Photoaffinity Analog with a 3-(4-benzoylphenyl)propanoyl Probe for Characterization of Drug-Binding Sites on Tubulin and P-Glycoprotein. *J. Med. Chem.* **1995**, *38*, 3891−3894.

(94) Liu, Y.; Ali, S. M.; Boge, T. C.; Georg, G. I.; Victory, S.; Zygmunt, J.; Marquez, R. T.; Himes, R. H. A Systematic SAR Study of C10 Modified Paclitaxel Analogues Using a Combinatorial Approach. *Comb. Chem. High Throughput Screening* **2002**, *5*, 39−48.

(95) Jimonet, P.; Ribeill, Y.; Bohme, G. A.; Boireau, A.; Chevé, M.; Damour, D.; Doble, A.; Genevois-Borella, A.; Herman, F.; Imperato, A.; Le Guern, S.; Manfré, F.; Pratt, J.; Randle, J. C. R.; Stutzmann, J.-M.; Mignani, S. Indeno[1,2-*b*]pyrazin-2,3-diones: A New Class of Antagonists at the Glycine Site of the NMDA Receptor with Potent in Vivo Activity. *J. Med. Chem.* **2000**, *43*, 2371−2381.

(96) Kuyper, L. F.; Baccanari, D. P.; Jones, M. L.; Hunter, R. N.; Tansik, R. L.; Joyner, S. S.; Boytos, C. M.; Rudolph, S. K.; Knick, V.; Wilson, H. R.; Caddell, J. M.; Friedman, H. S.; Comley, J. C. W.; Stables, J. N. High-Affinity Inhibitors of Dihydrofolate Reductase: Antimicrobial and Anticancer Activities of 7,8-Dialkyl-1,3-diaminopyrrolo[3,2-*f*]quinazolines with Small Molecular Size. *J. Med. Chem.* **1996**, *39*, 892−903.

JM060642I